

This is an electronic reprint of the original article.

This reprint *may differ* from the original in pagination and typographic detail.

Author(s): Katja T. Rinne-Garmston, Yu Tang, Elina Sahlstedt, Bartosz Adamczyk, Matthias Saurer, Yann Salmon, María del Rosario Domínguez Carrasco, Teemu Hölttä, Marco M. Lehmann, Lan Mo, Giles H. F. Young

Title: Drivers of intra-seasonal $\delta^{13}\text{C}$ signal in tree-rings of *Pinus sylvestris* as indicated by compound-specific and laser ablation isotope analysis

Year: 2023

Version: Publisher's version

Copyright: The author(s) 2023

Rights: CC BY 4.0





Rights url: <https://creativecommons.org/licenses/by/4.0/>

Please cite the original version:

Rinne-Garmston, K.T., Tang, Y., Sahlstedt, E., Adamczyk, B., Saurer, M., Salmon, Y. et al. (2023) Drivers of intra-seasonal $\delta^{13}\text{C}$ signal in tree-rings of *Pinus sylvestris* as indicated by compound-specific and laser ablation isotope analysis. *Plant, Cell & Environment*, 1–18

All material supplied via *Jukuri* is protected by copyright and other intellectual property rights. Duplication or sale, in electronic or print form, of any part of the repository collections is prohibited. Making electronic or print copies of the material is permitted only for your own personal use or for educational purposes. For other purposes, this article may be used in accordance with the publisher's terms. There may be differences between this version and the publisher's version. You are advised to cite the publisher's version.

Drivers of intra-seasonal $\delta^{13}\text{C}$ signal in tree-rings of *Pinus sylvestris* as indicated by compound-specific and laser ablation isotope analysis

Katja T. Rinne-Garmston¹  | Yu Tang^{1,2}  | Elina Sahlstedt¹ |
 Bartosz Adamczyk¹ | Matthias Saurer³  | Yann Salmon^{2,4}  |
 María del Rosario Domínguez Carrasco² | Teemu Hölttä² | Marco M. Lehmann³ |
 Lan Mo^{1,2} | Giles H. F. Young¹

¹Stable Isotope Laboratory of Luke (SILL), Natural Resources Institute Finland (Luke), Helsinki, Finland

²Institute for Atmospheric and Earth System Research (INAR)/Forest Sciences, Faculty of Agriculture and Forestry, University of Helsinki, Helsinki, Finland

³Forest Dynamics, Swiss Federal Institute for Forest, Snow and Landscape Research (WSL), Birmensdorf, Switzerland

⁴Institute for Atmospheric and Earth System Research (INAR)/Physics, Faculty of Science, University of Helsinki, Helsinki, Finland

Correspondence

Katja T. Rinne-Garmston, Stable Isotope Laboratory of Luke (SILL), Natural Resources Institute Finland (Luke), Helsinki, Finland.
 Email: katja.rinne-garmston@luke.fi

Funding information

European Research Council; Academy of Finland; Swiss National Science Foundation

Abstract

Carbon isotope composition of tree-ring ($\delta^{13}\text{C}_{\text{Ring}}$) is a commonly used proxy for environmental change and ecophysiology. $\delta^{13}\text{C}_{\text{Ring}}$ reconstructions are based on a solid knowledge of isotope fractionations during formation of primary photosynthates ($\delta^{13}\text{C}_{\text{P}}$), such as sucrose. However, $\delta^{13}\text{C}_{\text{Ring}}$ is not merely a record of $\delta^{13}\text{C}_{\text{P}}$. Isotope fractionation processes, which are not yet fully understood, modify $\delta^{13}\text{C}_{\text{P}}$ during sucrose transport. We traced, how the environmental intra-seasonal $\delta^{13}\text{C}_{\text{P}}$ signal changes from leaves to phloem, tree-ring and roots, for 7 year old *Pinus sylvestris*, using $\delta^{13}\text{C}$ analysis of individual carbohydrates, $\delta^{13}\text{C}_{\text{Ring}}$ laser ablation, leaf gas exchange and enzyme activity measurements. The intra-seasonal $\delta^{13}\text{C}_{\text{P}}$ dynamics was clearly reflected by $\delta^{13}\text{C}_{\text{Ring}}$, suggesting negligible impact of reserve use on $\delta^{13}\text{C}_{\text{Ring}}$. However, $\delta^{13}\text{C}_{\text{P}}$ became increasingly ^{13}C -enriched during down-stem transport, probably due to post-photosynthetic fractionations such as sink organ catabolism. In contrast, $\delta^{13}\text{C}$ of water-soluble carbohydrates, analysed for the same extracts, did not reflect the same isotope dynamics and fractionations as $\delta^{13}\text{C}_{\text{P}}$, but recorded intra-seasonal $\delta^{13}\text{C}_{\text{P}}$ variability. The impact of environmental signals on $\delta^{13}\text{C}_{\text{Ring}}$, and the 0.5 and 1.7‰ depletion in photosynthates compared ring organic matter and tree-ring cellulose, respectively, are useful pieces of information for studies exploiting $\delta^{13}\text{C}_{\text{Ring}}$.

KEYWORDS

CO_2 , phloem transport, photosynthesis: carbon reactions, stable carbon isotope ($\delta^{13}\text{C}$), sugars

This is an open access article under the terms of the Creative Commons Attribution License, which permits use, distribution and reproduction in any medium, provided the original work is properly cited.

© 2023 The Authors. *Plant, Cell & Environment* published by John Wiley & Sons Ltd.

1 | INTRODUCTION

Tree-ring stable carbon isotope record ($\delta^{13}\text{C}_{\text{Ring}}$) has become a commonly utilized proxy for environmental change and its impact on tree physiological processes (Helama et al., 2018; Kress et al., 2010; Rinne et al., 2010). At the same time, we do not yet fully understand the photosynthetic and post-photosynthetic metabolic processes and associated isotope fractionations leading to a specific $\delta^{13}\text{C}$ value of a xylem cell (Gessler et al., 2014; Schiestl-Aalto et al., 2021), or how the role of these individual processes may depend on the time of the growing season or changing environmental conditions. These unknowns affect the accuracy and spatial comparability of reconstructions that are based on the absolute $\delta^{13}\text{C}_{\text{Ring}}$ values, such as intrinsic water-use efficiency [iWUE, the ratio of photosynthetic rate (A) to stomatal conductance (g_s)] (Adams et al., 2020; Mathias & Thomas, 2021). They also exert a level of uncertainty for reconstructions that utilize the average $\delta^{13}\text{C}_{\text{Ring}}$ without the knowledge of how and why $\delta^{13}\text{C}$ varies within the analysed ring at a finer scale. Better knowledge of the processes that modify the $\delta^{13}\text{C}$ of leaf photosynthates ($\delta^{13}\text{C}_p$), such as sucrose and glucose, would also benefit studies interested in $\delta^{13}\text{C}$ of source and sink organ respiration (Barbour et al., 2005; Werner & Gessler, 2011; Wingate et al., 2010), carbon allocation dynamics in trees (Brüggemann et al., 2011; Tang, Schiestl-Aalto, Saurer, et al., 2022) or translocation of $\delta^{13}\text{C}_p$ signal belowground via ectomycorrhizal fungi (Hobbie et al., 2012; Högberg et al., 2010). This is because these processes are closely linked with $\delta^{13}\text{C}$ of sucrose ($\delta^{13}\text{C}_{\text{Suc}}$), which is the sugar transported from leaves to phloem and roots (Dennis & Blakeley, 2000).

A large uncertainty in using tree-ring carbon isotopes for environmental reconstructions is the potential reliance on carbohydrate reserves, which would uncouple $\delta^{13}\text{C}_{\text{Ring}}$ from its contemporary ambient environmental conditions. For broadleaved species, which can gain up to 30% of the total stem increment before budburst (Hinckley & Lassoie, 1981), the typical requirement of reserves for earlywood (EW) growth has been well demonstrated (Helle & Schleser, 2004) and, hence, their latewood (LW) section is normally used for environmental studies (Etien et al., 2009). Conifers, on the other hand, have several existing needle generations or, in the case of deciduous larch, bud burst typically occurs before the start of stem growth, providing fresh assimilates for cell formation (Rinne, Saurer, Kirilyanov, Loader, et al., 2015). Congruently, the studies that have followed $\delta^{13}\text{C}$ signal from bulk water-soluble carbohydrates (WSCs, $\delta^{13}\text{C}_{\text{WSC}}$) (*Pinus sylvestris*, Gessler, Brandes, et al., 2009) or individual sugars (*Larix gmelinii*, Rinne, Saurer, Kirilyanov, Loader, et al., 2015) (*P. sylvestris*, Tang et al., 2023) to $\delta^{13}\text{C}_{\text{Ring}}$ have found a close correspondence in intra-seasonal $\delta^{13}\text{C}$ trends between the two carbon pools. However, there is currently no consensus on the suitability of EW of boreal conifers for environmental studies (Fonti et al., 2018; Kagawa et al., 2006; Kress et al., 2009). Better knowledge of reserve use dynamics of conifers within a growing season could help to decipher whether there is the need to discard EW from environmental and tree physiological studies, such as reconstructions of iWUE (Michelot et al., 2011).

Additionally, the average $\delta^{13}\text{C}$ value of an annual ring and how well it represents the environmental conditions of that growing season are also dependent on other metabolic processes. These include isotope fractionation associated with activity of sucrose degrading invertase enzyme in leaves (Mauve et al., 2009; Rinne, Saurer, Kirilyanov, Bryukhanova, et al., 2015), potential isotope fractionation during phloem loading (Bögelein et al., 2019), mixing of sugar pools of different ages during phloem transport (Brandes et al., 2006) and isotope fractionation due to respiration (Gleixner et al., 1998) or during xylem formation (Panek & Waring, 1997). Although some of these processes have been examined relatively extensively in the literature (Gessler et al., 2014 and references therein), there are not many studies that have taken the analytical approach to compound-specific and high spatial and temporal resolution level (Rinne-Garmston et al., 2022; and references therein). The potential of identifying and quantifying the above listed processes is much better, if examining changes in $\delta^{13}\text{C}$ values of individual compounds, particularly of sugars, as opposed to $\delta^{13}\text{C}$ of a bulk matter, where the impact of a metabolic process may be obscured by the different metabolic history and biochemical role of the constituent compounds. This issue was demonstrated in Bögelein et al. (2019), where the absence of diel variation in $\delta^{13}\text{C}$ of leaf and twig phloem water-soluble organic matter of Douglas fir (*Pseudotsuga menziesii*) was assigned to the high content of isotopically invariable sugar alcohols in the bulk matter.

At leaf level, compound-specific isotope analysis (CSIA) has been applied in a few studies on WSCs of conifers, to examine how environmental signals are recorded and post-photosynthetically modified in $\delta^{13}\text{C}$ values of individual assimilates during a growing season (Rinne, Saurer, Kirilyanov, Bryukhanova, et al., 2015; Sidorova et al., 2018, 2019; Tang, Schiestl-Aalto, Lehmann, et al., 2022). In Rinne, Saurer, Kirilyanov, Loader, et al. (2015) the intra-seasonal records of needle $\delta^{13}\text{C}_{\text{Suc}}$ ($\delta^{13}\text{C}_{\text{Suc_Needle}}$) were further compared to high spatial resolution $\delta^{13}\text{C}_{\text{Ring}}$ profiles, to examine the reasons behind the widely reported ^{13}C -enrichment of sink organs relative to leaves (Gessler, Brandes, et al., 2009; Gleixner et al., 1993) and evaluate the quality of seasonal climate information stored in larch (*L. gmelinii*) trees. However, to our knowledge, there is no high spatial resolution CSIA data available for phloem, done together with intra-annual $\delta^{13}\text{C}_{\text{Ring}}$ profiling, so that it could be possible to separate the impact of individual metabolic processes on $\delta^{13}\text{C}_{\text{Suc}}$ along its transport route from leaves to stem xylem. The preexisting CSIA studies have focused either on examining carbon allocation patterns with the $^{13}\text{CO}_2$ -labelling technique (Galiano et al., 2017; Streit et al., 2013), which has the drawback of losing the environmental and physiological information recorded in $\delta^{13}\text{C}$ variability at natural abundance, or on studying biosynthetic pathways and isotope fractionations within a very narrow timeframe (Bögelein et al., 2019; Smith et al., 2016). Several studies have, though, examined down-stem isotope fractionations using phloem sap (Gessler et al., 2004), but reached contradictory outcomes on, for example, the occurrence of a ^{13}C -fractionation process during xylem formation (Cernusak et al., 2005; Gessler, Brandes, et al., 2009). Although sucrose is the

main constituent, phloem sap contains also a variable amount of other sugars, such as glucose (Devaux et al., 2009), and other compounds (Merchant et al., 2010) with distinctive $\delta^{13}\text{C}$ values (Bögelein et al., 2019). Hence, there is a factor of uncertainty connected with the utilization of phloem sap for isotope fractionation studies.

In this paper, we examine the environmental signal recorded in leaf $\delta^{13}\text{C}_{\text{Suc}}$ and how it is kept along sucrose transport pathway to phloem, tree-rings and roots. It aims to resolve some of the controversy concerning the significance of the individual metabolic processes in the post-photosynthetic modification of isotopic signal and to quantify their impact on $\delta^{13}\text{C}$. With the aid of CSIA data, it also studies the quality of environmental and tree physiological signal in $\delta^{13}\text{C}_{\text{WSC}}$, and potential issues when using WSCs for isotope measurements. The study was conducted at controlled, regularly watered conditions for clones of 7-year-old *P. sylvestris* L. saplings, in which $\delta^{13}\text{C}_{\text{Ring}}$ profiles were time-scaled by sampling the ring during growth, concurrently with sampling of leaves, phloem and roots for carbohydrate $\delta^{13}\text{C}$ analysis. Specifically, we seek answers to the following questions: (1) What is the impact of the postulated isotope fractionation and mixing processes occurring during phloem loading on $\delta^{13}\text{C}_{\text{Suc}}$? (2) What processes modify phloem $\delta^{13}\text{C}_{\text{Suc}}$ before its use to produce tree-ring material and to what extent? (3) What is the isotopic offset between leaf sugars and tree-rings? Further, this unique data set enables us to estimate the sensitivity of $\delta^{13}\text{C}_{\text{WSC}}$ to environmental changes and its suitability for determining post-photosynthetic fractionation processes. This detailed data set also allows us to evaluate the impact of reserve use on EW $\delta^{13}\text{C}$. These questions are tackled with an exceptionally diverse data set that combines for the first time intra-seasonal analysis of $\delta^{13}\text{C}_{\text{Suc}}$, glucose $\delta^{13}\text{C}$ ($\delta^{13}\text{C}_{\text{Glc}}$) and $\delta^{13}\text{C}_{\text{WSC}}$ in leaves, phloem and roots with intra-ring $\delta^{13}\text{C}$ profiling from laser ablation isotope ratio mass spectrometry (LA-IRMS). The data interpretations were supported by leaf gas exchange measurements and leaf starch analysis, and analysis of enzymes involved in sucrose synthesis and degradation in leaves, to better understand how the invertase-related fractionation is manifested in $\delta^{13}\text{C}$ values of leaf sugars (Gilbert et al., 2011).

2 | MATERIALS AND METHODS

2.1 | Plant material and experimental setup

The experiment was conducted during summer 2018 in a greenhouse of University of Helsinki (60°14'N, 25°01'E). The 7-year-old saplings of *P. sylvestris* were obtained in May 17, at the beginning of the growing season (May 22 ± 13 days in Jyske et al., 2014), in 2018 from outdoor nursery garden of Haapastensyrjä (60°37'N, 24°27'E). Four different clones (clones A, B, C and D in Supporting Information: Figure S1) of *P. sylvestris* were available for the study (for more details, see Ryhti et al., 2022). Nine specimens of each four clones (i.e., 36 saplings in total) were dug-out with their roots and the attached soil (below-ground volume was ~3.5 L) for immediate

transport. The average temperature (T) of May was 14.6°C in Haapastensyrjä, where the saplings had grown in open air, and 21.6°C in the greenhouse. Clones were used to minimize the non-environmentally driven temporal variability in the analytical results (Schuster et al., 1992), a beneficial approach for studies using destructive sampling (see Section 2.2). Four clones, instead of a single clone, were used and their measurements (e.g., $\delta^{13}\text{C}$) averaged for each sampling day, to obtain results that better represent the studied species rather than responses of an individual (Leavitt & Long, 1984).

At the greenhouse in Helsinki, the saplings were repotted in May 17 into 7.5 L pots and filled with additional peat-based soil. At the start of the experiment, stem diameter (near soil surface) was 21 ± 5, 21 ± 4, 21 ± 4 and 18 ± 3 mm, and the height of the saplings (from the soil surface) was 120 ± 17, 113 ± 15, 104 ± 13 and 96 ± 10 cm, for clones A, B, C and D, respectively. The saplings of each clone were distributed randomly on a table with automated watering system to maintain the plants at well-watered conditions. The watering was used each Tuesday, Thursday, Saturday and Sunday for a period of 15 min. To assure equal light conditions for each sapling during the experiment, the position of each tree on the table was changed every second day.

2.2 | Sampling and instrumental measurements

Destructive sampling was done between 1300 and 1700 h once a week from June 5 to July 30. On each sampling day, one sapling from each four group of clones (A, B, C and D) was randomly selected for analysis (Supporting Information: Figure S1). Immediately before the sampling, leaf gas-exchange measurements were conducted on 1-year-old needles (1 N). A, g_s and leaf internal concentration of CO_2 (c_i) were measured using a GFS-3000 (Heinz Walz GmbH). The conditions inside the measurement cuvette (T, photosynthetically active radiation, vapour pressure deficit (VPD) and CO_2 concentration) were set to track ambient conditions in the greenhouse. Sampling of 1 N, current-year needles (0 N), stem phloem and roots was conducted for analysis of WSCs. Needles were collected from several branches around the canopy to ensure representative results. Phloem, including cambium and periderm, was obtained by removing the outer bark and by separating the xylem on the basis of differences in hardness and colour (Lintunen et al., 2016). The samples were immediately placed in a cool box with ice blocks, and treated in a microwave within 2 h of collection to stop metabolic activities (Wanek et al., 2001). The samples were subsequently dried for 24 h at 60°C, and ground to fine powder. On sampling days between June 18 and July 23, 0 and 1 N were additionally collected for determining activity of the enzymes involved in sucrose synthesis and degradation. These samples were immediately snap-frozen on dry ice and stored in -80°C before analyses. Finally, the stem of each sampled tree was micro-cored with a Trephor instrument (Rossi et al., 2006) for xylogenesis observations, and the obtained sample was placed in ethanol-water solution (1:1). The remaining stem was dried and stored in room T for $\delta^{13}\text{C}$ analysis of resin extracted

tree-ring ($\delta^{13}\text{C}_{\text{Ring_RE}}$). T and relative humidity (RH) were automatically recorded at 15 min intervals with thermo- and psychrometer (Priva Hortimation). They averaged 23.3°C and 56%, respectively, for the study period.

2.3 | Intra-annual tree-ring $\delta^{13}\text{C}$ analysis

A disk was cut from all stems, approximately 10 cm above soil surface, collected on June 5 (the first sampling day), July 2 and July 30 (the last sampling day), to establish a time-axis for $\delta^{13}\text{C}_{\text{Ring_RE}}$ profiles. The disks were treated in a Soxhlet apparatus with ethanol for 48 h to remove resins and other soluble materials. Subsequently, ethanol was removed by boiling the disks for 6 h in water, which was replaced every hour, and the disks were dried at 40°C in an oven for 2 day. The samples were then sanded for a smooth, even surface with a series of finer sandpapers until all cells were clearly visible under magnification before LA-IRMS analysis of year 2018. Any remaining wood powder from sanding was removed in an ultrasonic bath in water, and the samples were dried once more.

One approximately 5 mm wide segment was cut from the resin extracted disks of July 30 for determining the difference in $\delta^{13}\text{C}$ values between resin extracted wood and tree-ring α -cellulose ($\delta^{13}\text{C}_{\text{Ring_Cellulose}}$). From these segments, the EW and LW of 2018 were separated with a scalpel into small slivers. A representative subsample was taken from each EW and LW sample for EA-IRMS $\delta^{13}\text{C}$ analysis. The remaining slivers were extracted to α -cellulose, a procedure which involves removal of lignins by treatment with acidic sodium chlorite solution, and treatment with first 10% and then 17% sodium hydroxide solution to leach hemicelluloses (Loader et al., 1997; Rinne et al., 2005).

High spatial resolution $\delta^{13}\text{C}$ profiles were determined for resin extracted wood ($\delta^{13}\text{C}_{\text{Ring}}$) by LA-IRMS analysis at Stable Isotope Laboratory of Luke (SILL), Finland. The operational principle was as described in Tang et al. (2023), based on Schulze et al. (2004) and Loader et al. (2017). In brief, the LA-IRMS analysis consists of sampling a tree-ring by laser ablation (LSX-213 G+; Teledyne Photon Machines), combustion of the formed wood powder to CO_2 in a glass reactor tube (OD = 6 mm) filled with Cr_2O_3 and held at 700°C, collection of the CO_2 in a liquid nitrogen trap, and finally heating of the trap to room temperature, which releases the CO_2 to IRMS (Sercon 20-22; Sercon Ltd.) for $\delta^{13}\text{C}$ analysis. Water produced in the combustion reaction is separated from the sample stream using a Nafion™ drying tube downstream of the reactor. The laser parameters are operated and automated sampling sequences are created via a separate software (Chromium; Teledyne Photon Machines). In this study, we analysed tree-rings at 40 μm (40 μm wide tracks placed in a zig-zag pattern, 'third LA series' in Figure 1) or 80 μm (40 μm wide tracks with 40 μm spacing, 'first LA series' in Figure 1) resolution, starting from the beginning of the annual ring and ending to the bark edge. 'Raw' $\delta^{13}\text{C}$ values, which were calculated by the IRMS software (Callisto; Sercon Ltd.) by comparison to reference CO_2 gas pulses with a known $\delta^{13}\text{C}$, were calibrated against a USGS-55 (Mexican ziricote wood, -27.13‰) and an in-house (yucca tree powder, -15.46‰) reference materials (powders compressed to solid pellets by manual hydraulic press). The calibration standards were placed with the samples into the laser chamber and analysed concurrently with LA-IRMS. IAEA-C3 cellulose paper was also measured concurrently with the samples and similarly calibrated against the USGS-55 and in-house references, thus giving an average $\delta^{13}\text{C}$ value of -24.81 ± 0.16 (n = 113), which agrees well

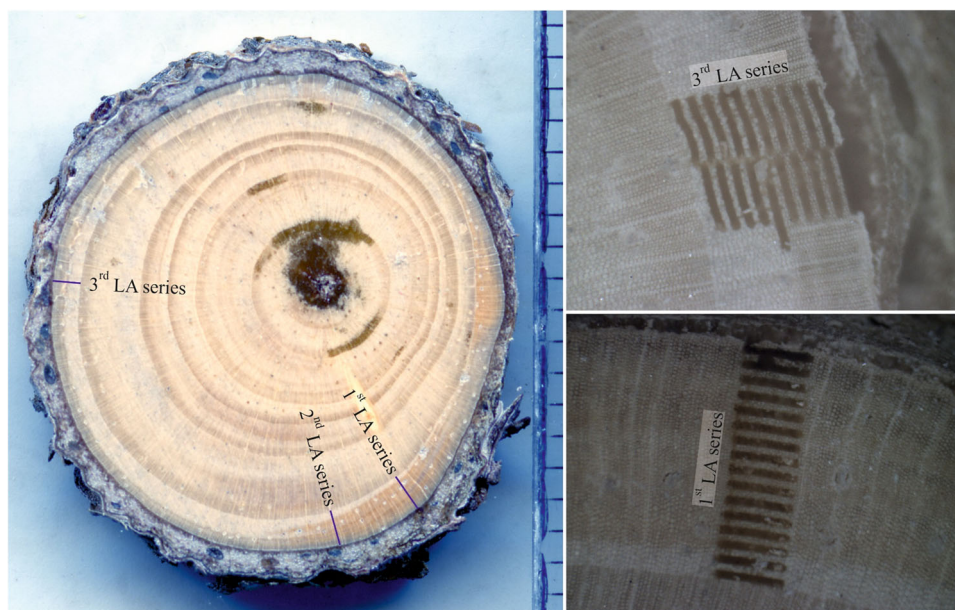


FIGURE 1 Disk sections of *Pinus sylvestris* examined for clone B of July 30 using LA-IRMS. The first and second $\delta^{13}\text{C}$ series contained compression wood (CW) whereas the third series was on normal density wood. The $\delta^{13}\text{C}$ profiles are shown in Figure 2. LA-IRMS, laser ablation isotope ratio mass spectrometry.

with the values reported for this material: $-24.91 \pm 0.49\%$ (IAEA-C3, cellulose paper) and $-24.72 \pm 0.04\%$ (IAEA-CH3, powder prepared from IAEA-C3). Signal size effects on $\delta^{13}\text{C}$ were monitored and, when necessary, corrected for by running a set of reference sample laser lines at different lengths and spot sizes to produce variable signal sizes.

2.4 | Alignment and time-scaling of tree-ring $\delta^{13}\text{C}$ profiles

Intra-annual low frequency $\delta^{13}\text{C}$ variability was similar for the analysed tree-ring sections, enabling the alignment of the $\delta^{13}\text{C}_{\text{Ring_RE}}$ series and, hence, time-scaling of the profiles. The June 5 series were used to identify, which section of the July 30 $\delta^{13}\text{C}$ profiles were formed before the start of the experiment, and July 2 tree-ring group was used to determine which part of July 30 series had formed by July 2. Thereafter, phloem sugar $\delta^{13}\text{C}$ series were incorporated together with $\delta^{13}\text{C}_{\text{Ring_RE}}$ series into Figure 2 using the common sampling days (June 5, July 2 and July 30), and used to finalize the time-scaling of the x-axis. The detailed description of the alignment procedure is given in the Supporting Information: Method S1.

2.5 | Extraction and purification of sugars and starch

Water soluble compounds in 0, 1 N, phloem and roots were extracted using a modified method after Wanek et al. (2001). Two microlitres reaction vials were filled with 60 mg of homogenized plant powder and 1.5 mL of Milli-Q water, stirred with vortex, and placed in a water bath at 85°C for 30 min. Once the samples had cooled down, they were centrifuged at 10 000 g for 2 min. WSCs were isolated from the supernatant using three types of sample treatment cartridges, as described in Rinne et al. (2012). The WSC-samples were then freeze-dried, dissolved in 1 mL of Milli-Q water, pressed through a 0.45 μm syringe filter.

For 1 N, starch was extracted from the pellet of the WSC extraction by enzymatic hydrolysis (Lehmann et al., 2019; Wanek et al., 2001). Shortly, pellet in each reaction vial was washed repeatedly with 1.2 mL methanol-chloroform-water (12:5:3, v/v/v) solution for lipid removal, followed by washes with deionized water. Subsequently, starch in each pellet was gelatinized at 99°C for 15 min and hydrolysed with purified (with Vivaspin 15R; Sartorius) α -amylase (EC 3.2.1.1; Sigma-Aldrich) solution at 85°C for 2 h. Hydrolysed starch in supernatant was cleaned with centrifugation filters (Vivaspin 500; Sartorius). Identical treatment principle (Werner & Brand, 2001) was applied to two maize starch standards (Fluka), two wheat starch standards (Fluka) and four blanks with every batch of 40 samples. The WSC and starch samples were stored in a -20°C freezer until further use.

2.6 | CSIA of sugars with HPLC-IRMS

The WSC extracts were analysed online using a Delta V Advantage IRMS coupled with HPLC with a Finnigan LC Isolink interface (Krummen et al., 2004; Rinne et al., 2012) at WSL, Switzerland. A column T of 20°C (CarboPac PA20; Thermo Fisher Scientific) was used to prevent isomerization of hexoses with 1% NaOH as the HPLC eluent (Rinne et al., 2012). Excellent chromatographic peak separation and peak shape were obtained for sucrose and glucose of the analysed extracts (Supporting Information: Figure S2). Fructose was excluded from further analysis, because its $\delta^{13}\text{C}$ value was affected by peak tailing and occasional co-elution with another compound under these analytical settings (Rinne et al., 2012). Furthermore, glucose and fructose are often isotopically similar and, hence, there may not be an added benefit of obtaining fructose $\delta^{13}\text{C}$ values for studying post-photosynthetic fractionations (Rinne-Garmston et al., 2022). All extracts also contained a significant amount of sugar alcohols pinitol/myo-inositol ('pinitol' from now on, Supporting Information: Figure S2), which co-elute from the column. A dilution series (20, 40, 60, 90, 120 and 180 $\text{ng C}\mu\text{L}^{-1}$) of external compound-matched standard solutions (mixture of sucrose, glucose, fructose and pinitol) were analysed between every 10 samples to correct sample $\delta^{13}\text{C}$ values (Rinne et al., 2012). The standard deviation of the repeated analytical measurements was 0.31‰ for sucrose (-25.37%) and 0.51‰ (-10.24%) for glucose standards.

2.7 | $\delta^{13}\text{C}$ and concentration analysis with EA-IRMS

The 1 N starch extracts in liquid were pipetted into tin capsules and freeze-dried. The dry resin-extracted and cellulose-extracted samples of tree-rings, and WSCs were weighted into tin capsules (IVA Analysentechnik). The samples were analysed for $\delta^{13}\text{C}$ using an elemental analyser (Europa EA-GSL; Sercon Limited) coupled to an IRMS (Sercon Limited) at SILL, Finland. The $\delta^{13}\text{C}$ values were calibrated against IAEA-CH3 (cellulose, -24.72%), IAEA-CH7 (polyethylene, -32.15%) and an in-house (sucrose, -12.22% and lactose, -24.66%) reference materials. Measurement precision was 0.1‰ (SD), determined from repeated measurements of a quality control material.

Starch concentrations were determined using the weight of starch in tin capsules and the weights of plant materials used for extraction, and by considering a conversion factor for the efficiency of the enzymatic conversion of starch to hydrolysed glucose (Tang, Schiestl-Aalto, Lehmann, et al., 2022). The blanks used in starch extraction contained residuals of α -amylase, having $\delta^{13}\text{C}$ value of $-27.62 \pm 0.63\%$. Blank concentration was on average $0.14 \pm 3 \text{ mg/mL}$ in the final extraction solution. Sample to the average blank amount ratio was often 2 or less, causing significant uncertainty on the 1 N starch $\delta^{13}\text{C}$ results. The impact of blank correction on $\delta^{13}\text{C}$ values is illustrated in Figure 3.

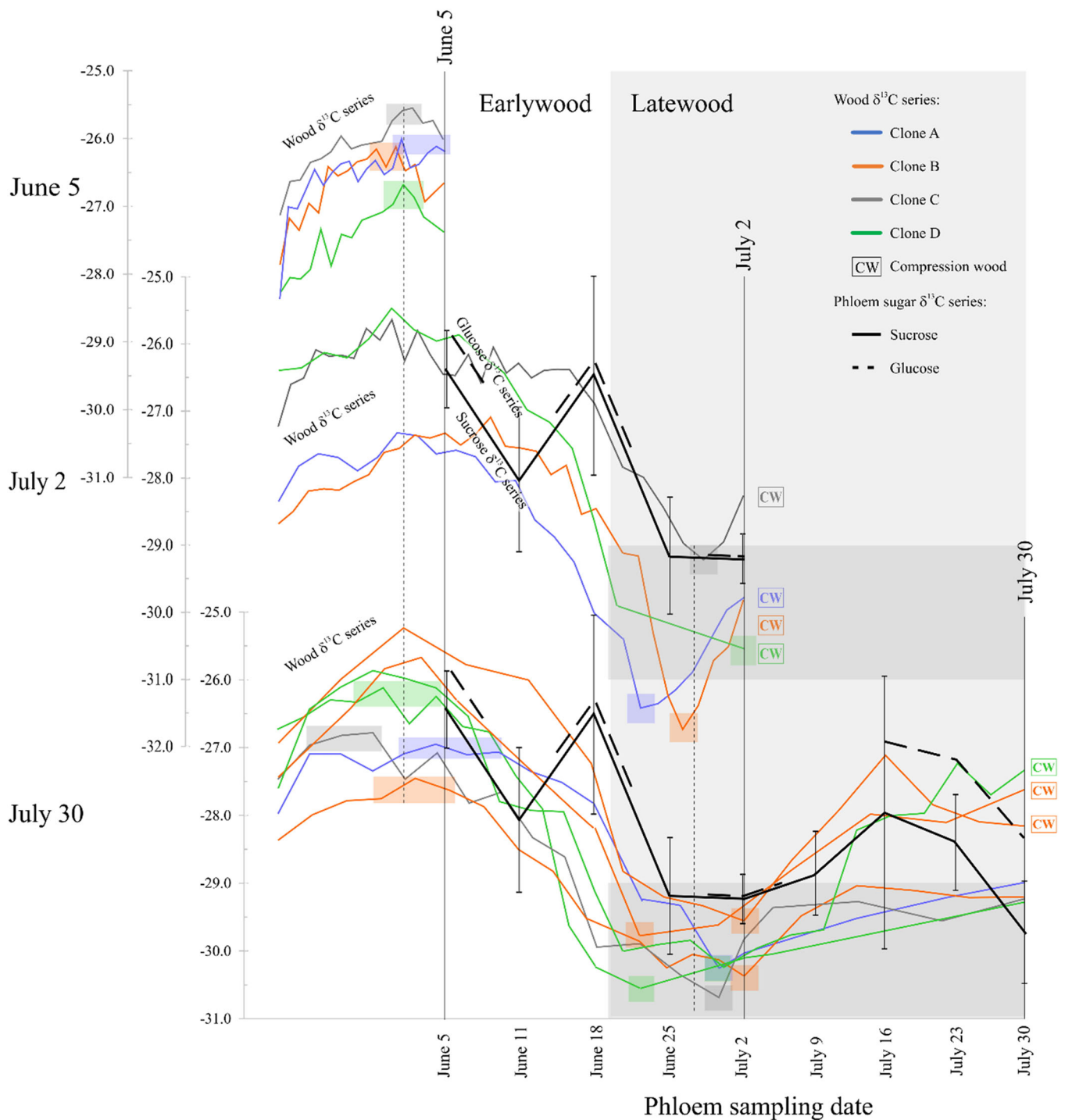


FIGURE 2 Intra-annual $\delta^{13}\text{C}$ composition of tree rings and seasonal changes in $\delta^{13}\text{C}$ of phloem sugars of *Pinus sylvestris* saplings. The dates on the y-axis divide the series into three groups based on the sampling day of the saplings for tree ring $\delta^{13}\text{C}$ analysis. June 5 tree ring $\delta^{13}\text{C}$ series represent the xylem wood formed before the start of the experiment. July 2 tree ring $\delta^{13}\text{C}$ series represent the wood formed by July 2, and July 30 series the wood formed by the end of the experiment. The coloured squares are the three maximum or one minimum values of wood $\delta^{13}\text{C}$ series, and were used to align the wood $\delta^{13}\text{C}$ series of June 5, July 2 and July 30 (see Supporting Information: Method S1). Earlywood (EW) and latewood (LW) areas and indicated. The darker LW bands indicate $\delta^{13}\text{C}$ values between -29 and -31% , to enhance visual comparisons. Some of the wood $\delta^{13}\text{C}$ series were analysed on compression wood (CW) to obtain more $\delta^{13}\text{C}$ datapoints for LW. Each phloem $\delta^{13}\text{C}$ value represents the average of four clones (A–D) and the error bars its standard deviations.

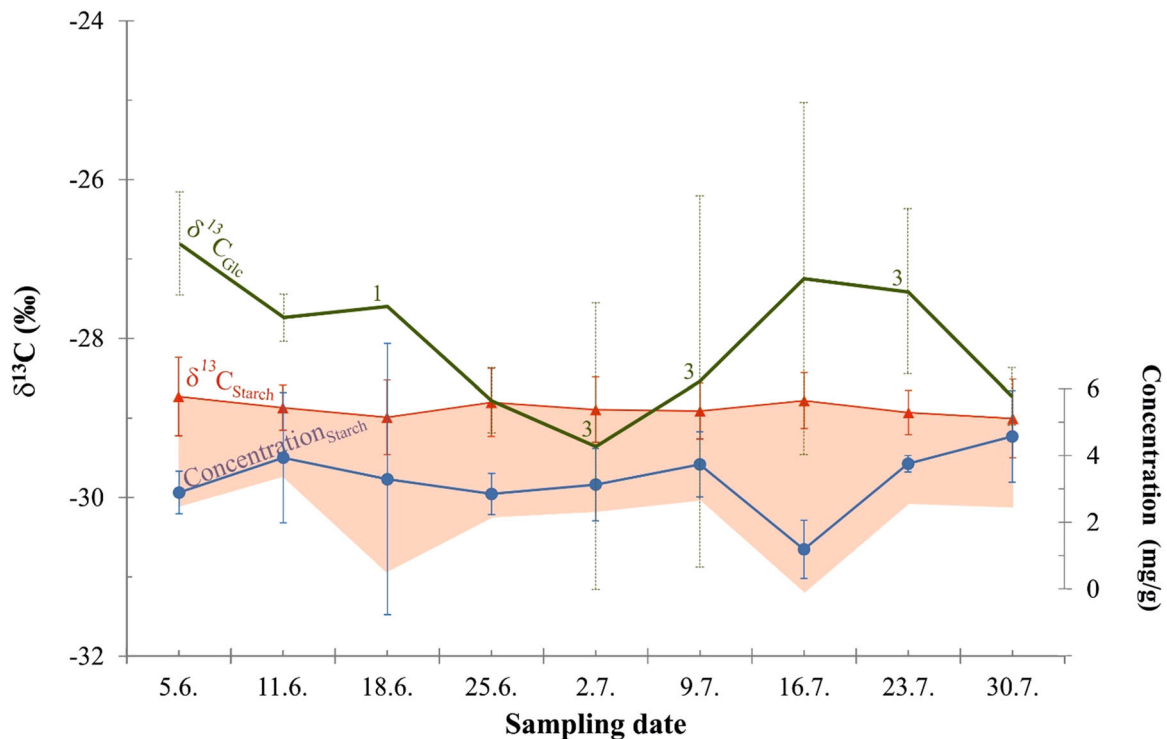


FIGURE 3 Measured $\delta^{13}\text{C}$ and concentration of starch, and $\delta^{13}\text{C}$ of glucose of 1-year-old needles of *Pinus sylvestris* saplings. For starch, each data point represents the average of four trees and the error bars its standard deviations (clones A, B, C and D). Glucose content was too low in some samples for accurate $\delta^{13}\text{C}$ measurements. A number in the figure indicates the replication when $n < 4$ for the calculated $\delta^{13}\text{C}$ average. For starch, the impact of blank correction on $\delta^{13}\text{C}$ (^{13}C -depletion of values) is indicated by the red shaded area.

2.8 | Determination of enzyme activities for needles

Enzymes were extracted as described in Nguyen et al. (2016) and Rende et al. (2017). Briefly, 250 mg of needles were ground in liquid nitrogen. Enzymes were extracted with 50 mM HEPES buffer, pH 8, with 1 mM EDTA, 10 mM MgCl_2 , 1 mM EGTA, 5 mM dithiothreitol, 1 mM PMSF, 1% TritonX-100, 2% glycerol and 3% PVPP. Following centrifugation (5 min, 14 000 g), supernatants were filtered using VWR centrifugal filters with 10 K MWCO. Filtered extract was used to measure activity of sucrose forming and degrading enzymes.

Invertase activity was measured as described in Jammer et al. (2015). Briefly, filtered extracts (20 μL) were incubated at 37°C for 30 min with 5 μL of 100 mM sucrose and 5 μL 0.4 M reaction buffer of pH 4.5 or pH 6.8 for acid invertase (INV_{acid}) and neutral invertase ($\text{INV}_{\text{neutral}}$), respectively. For control reactions, sucrose was omitted. The amount of liberated glucose from sucrose was determined by measurement of absorbance at 405 nm in a plate reader (CLARIOstar; BMG Labtech) after 30 min incubation at room T with 200 μL of glucose oxidase-peroxidase reagent, and 0.8 mg mL^{-1} ABTS in 0.1 M potassium phosphate buffer pH 7.0. Standard curve was made on the basis of known concentration of glucose. Enzymatic activities are given as nmol of glucose per hour per dry weight of needles.

Activity of sucrose synthase was measured as described in Nguyen et al. (2016). Briefly, sucrose-degrading SuSy ($\text{SuSy}_{\text{degradation}}$)

activity was measured by adding 25 μL filtered extract to 200 μL of solution with 10 mM sucrose and 10 mM UDP (uridine 5'-diphosphate), pH 5.0 followed by 1 h incubation at 37°C. The same reaction, but with no UDP, was conducted to estimate sucrose-degrading activity caused by other enzymes existing in filtered extract. Sucrose-synthetizing SuSy ($\text{SuSy}_{\text{synthesis}}$) activity was measured by adding 25 μL filtered extract to 200 μL solution with 10 mM UDP-glucose and 10 mM fructose, pH 5.0 followed by 1 h incubation at 37°C. Controls did not include extract. Fructose reacted with 0.25% triphenyltetrazoliumchloride (TTC) in 1 M NaOH producing red colour measured at 495 nm at microplate reader (CLARIOstar; BMG Labtech). Standard curve was based on known concentration of fructose. Enzymatic activities are given as nmol of fructose per hour per dry weight of needles. However, the use of plant extract with no in-depth enzyme purification, like in our study, does not enable to clearly differentiate between sucrose phosphate synthase and SuSy (sucrose forming) activities and, hence, $\text{SuSy}_{\text{synthesis}}$ represents the activity of both sucrose-forming enzymes.

2.9 | Data analysis

CorelDRAW Graphics Suite X7 was used for aligning the LA-IRMS $\delta^{13}\text{C}$ series. IBM SPSS Statistics software package was used for correlation analysis, where the average values of the four clones

were used, and for two-sample *t*-tests. *i*WUE was calculated from the gas exchange data as the ratio between *A* and *g_s*. $\delta^{13}\text{C}$ of primary photosynthates was calculated ($\delta^{13}\text{C}_{\text{P-cal}}$) by the classic photosynthetic discrimination model (Supporting Information: Method S2; Farquhar et al., 1982, 1989) using the gas exchange data of 1 N as input.

3 | RESULTS

3.1 | Water status and gas exchange

VPD measured at 1400 h varied from 9.05 to 42.5 hPa between the sampling days (Figure 4), and *T* from 21.6°C to 35.7°C. Although the studied trees received regular watering, they were affected by water limitations, when VPD was high. This was indicated by an inverse relationship between VPD and *A* or *g_s* of trees, when VPD was at maximum (June 11, June 18 and July 16, Figure 4). Due to this inconsistent relationship between these parameters, VPD did not

correlate with *A* or *g_s* for the entire study period. *i*WUE, from the gas exchange data, first declined until July 2, followed by a sharp increase, and a subsequent general decline until the end of the experiment (Figure 4).

3.2 | $\delta^{13}\text{C}_{\text{Suc}}$, $\delta^{13}\text{C}_{\text{Glc}}$ and $\delta^{13}\text{C}_{\text{WSC}}$ in studied organs

The temporal variation of $\delta^{13}\text{C}_{\text{Suc}}$ was similar for 0, 1 N, phloem and roots (Table 1), but there were significant isotopic offsets between the organs (Figure 5 and Table 2). The organ specific ^{13}C -enrichment of sucrose was as following: 0 N < 1 N = phloem < roots, where the $\delta^{13}\text{C}$ offsets were $1.2 \pm 0.8\text{‰}$ [0 N vs. phloem, $t(62) = 2.743$, $p < 0.008$] and $1.0 \pm 0.5\text{‰}$ [phloem vs. roots, $t(68) = 2.809$, $p < 0.006$] (Table 2). When considering that 0 N contained on average 1.5 times more sucrose than 1 N, the ^{13}C -enrichment of phloem over the two needle generations was $0.7 \pm 1.0\text{‰}$ according to mass balance calculation (Table 2, see also Section 3.3. for needle enzyme activity).

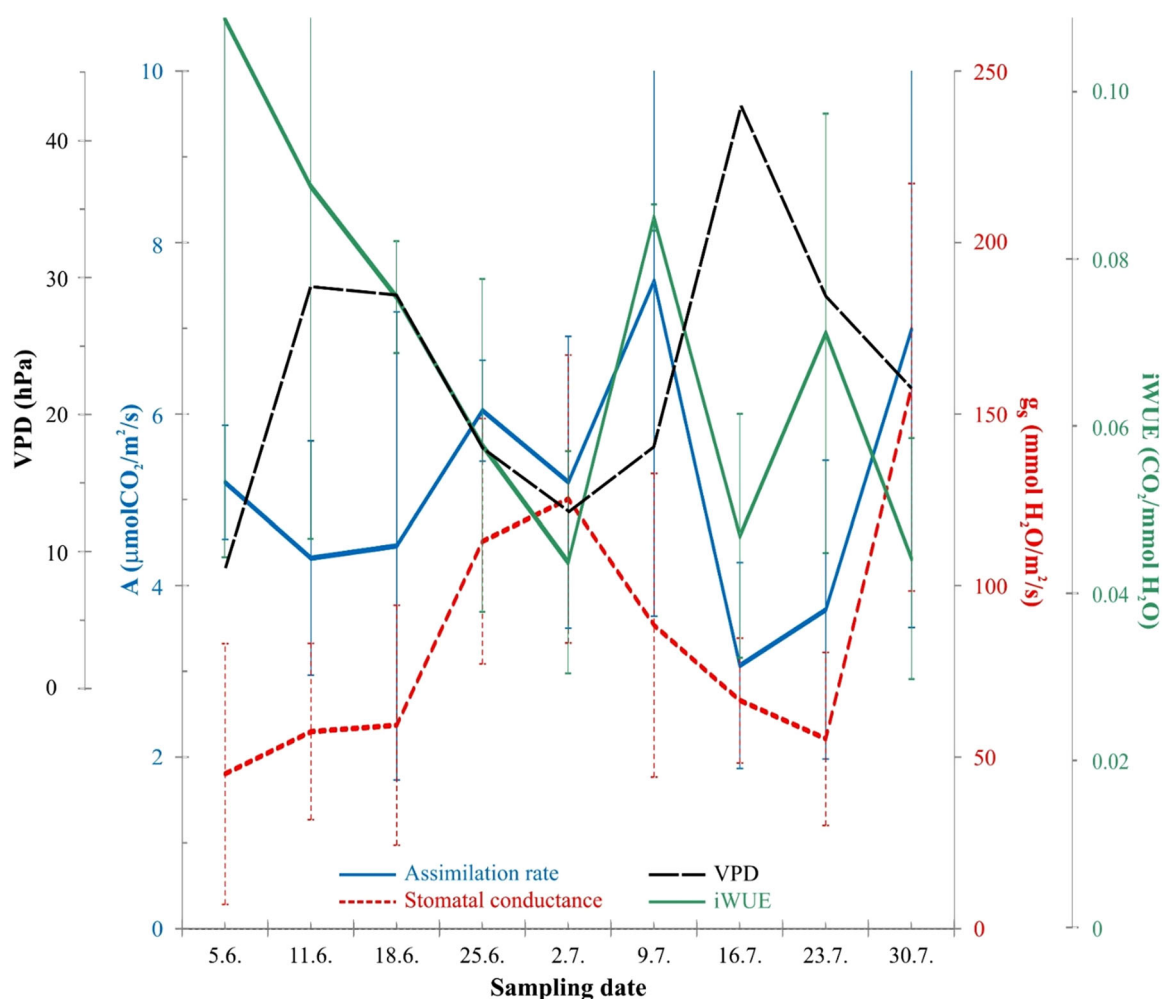


FIGURE 4 Changes in assimilation rate (*A*), stomatal conductance (*g_s*) and intrinsic water-use efficiency (*i*WUE) of *Pinus sylvestris* with vapour pressure deficit (VPD) during the study period. Each gas exchange measurement value represents the average of four clones (A–D) and the error bars its standard deviations.

TABLE 1 The results of correlation analysis (r -values) for sucrose, glucose and water-soluble carbohydrate (WSC) $\delta^{13}\text{C}$ in different organs of *Pinus sylvestris*, photosynthetic parameters, climate parameters and calculated $\delta^{13}\text{C}$ of primary photosynthates ($\delta^{13}\text{C}_{\text{P_calc}}$) from leaf gas exchange measurements.

	$\delta^{13}\text{C}_{\text{Suc}}$				Photosynthetic parameters				Climate parameters		
	0 N	1 N	Phloem	Roots	A	g_s	$\delta^{13}\text{C}_{\text{P_calc}}$	iWUE	VPD	RH	T
$\delta^{13}\text{C}_{\text{Suc}}$	0 N ($n = 9$)	0.79 ^a	0.79 ^a	0.78 ^a	-0.67 ^a	-0.76 ^a	0.60 (0.75 ^a)	0.44 (0.66)	0.45	-0.70 ^a	0.35
	1 N ($n = 9$)		0.50	0.48	-0.51	-0.56	0.52 (0.54)	0.34 (0.38)	0.46	-0.42	0.50
	Phloem ($n = 9$)			0.91 ^b	-0.49	-0.83 ^b	0.77 ^a (0.81 ^a)	0.67 ^a (0.76 ^a)	0.11	-0.77 ^a	-0.17
	Roots ($n = 9$)				-0.32	-0.71 ^a	0.80 ^b (0.86 ^b)	0.65 (0.77 ^a)	0.22	-0.82 ^b	0.05
$\delta^{13}\text{C}_{\text{Glu}}$	0 N ($n = 9$)	0.91 ^b			-0.52	-0.67 ^a	0.59 (0.74 ^a)	0.47 (0.71)	0.24	-0.73	0.10
	1 N ($n = 9$)		0.75 ^a		-0.62	-0.86 ^b	0.72 ^a (0.86 ^b)	0.59 (0.82 ^b)	0.38	-0.73 ^a	0.27
	Phloem ($n = 6$)			0.89 ^b	-0.39	-0.85 ^a	0.95 ^b (1.00 ^b)	0.82 ^a (0.93 ^a)	0.15	-0.78	0.02
	Roots ($n = 8$)				0.81 ^a	-0.54	-0.71 ^a	0.70 (0.72)	0.50 (0.54)	0.55	-0.71 ^a
$\delta^{13}\text{C}_{\text{WSC}}$	0 N ($n = 9$)	0.52			-0.26	-0.70 ^a	0.65 (0.77 ^a)	0.61 (-0.82 ^a)	0.00	-0.76 ^a	-0.30
	1 N ($n = 9$)		0.24		-0.31	-0.86 ^b	0.84 ^b (0.90 ^b)	0.76a (-0.88 ^b)	0.15	-0.84 ^b	-0.14
	Phloem ($n = 9$)			0.82 ^b	-0.35	-0.80 ^b	0.77 ^a (0.84 ^b)	0.59 (0.71 ^a)	0.30	-0.67	0.12
	Roots ($n = 9$)				0.82 ^b	-0.52	-0.69 ^a	0.69 ^a (0.74 ^a)	0.54 (0.63)	0.29	-0.66

Note: The studied organs included current-year needles (0 N), one-year-old needles (1 N), phloem and roots. The determined photosynthetic and climate parameters were assimilation rate (A), stomatal conductance (g_s), gas-exchange derived $\delta^{13}\text{C}$ value of primary photosynthates ($\delta^{13}\text{C}_{\text{P_calc}}$) gas-exchange derived intrinsic water-use efficiency (iWUE), vapour pressure deficit (VPD), relative humidity (RH) and temperature (T). The r -values and significance levels (^a95% significance level, ^b99% significance level) are shown. The r -values in brackets were obtained, when the data of July 16 (VPD maxima) was excluded. The correlation between $\delta^{13}\text{C}_{\text{P_calc}}$ and leaf-internal concentration of CO_2 (c_i) with iWUE was -0.98 ($p < 0.01$).

Abbreviation: WSC, water-soluble carbohydrate.

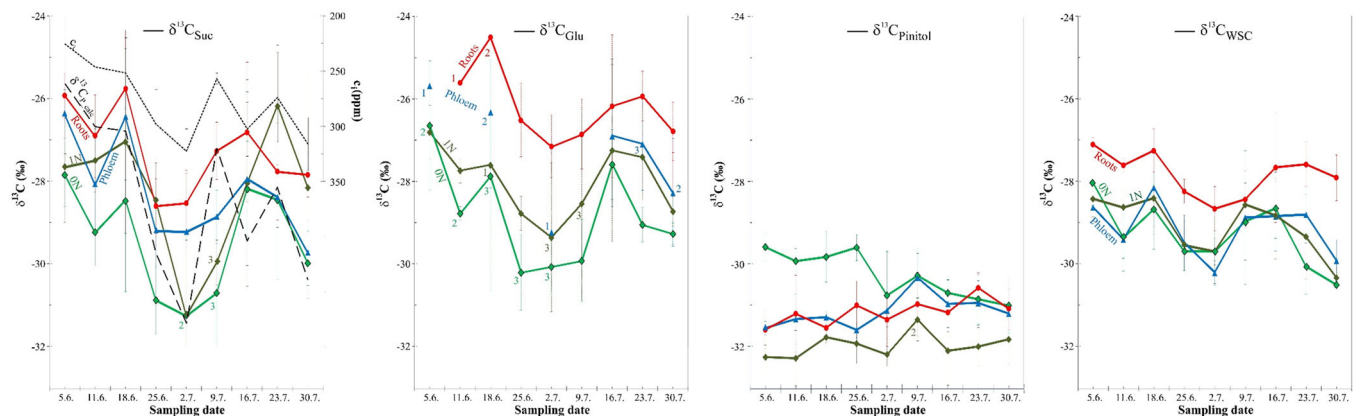


FIGURE 5 Comparison of sucrose, glucose, pinitol and water-soluble carbohydrate (WSC) $\delta^{13}\text{C}$ values in different tree organs with leaf internal concentration of CO_2 (c_i , reversed y-axis scale) and calculated $\delta^{13}\text{C}$ of primary photosynthates ($\delta^{13}\text{C}_{\text{P_calc}}$) from gas exchange measurements of *Pinus sylvestris*. For the gas exchange, 1-year-old needles (1 N) were used. 0 N is current-year needles. In general, each sucrose and WSC $\delta^{13}\text{C}$ value represent the average of four clones (A–D) and the error bars its standard deviations. Glucose content was too low in several samples for accurate CSIA. A number in the figure indicates the replication when $n < 4$ for the calculated $\delta^{13}\text{C}$ average. CSIA, compound-specific isotope analysis.

$\delta^{13}\text{C}_{\text{Glc}}$ series correlated with $\delta^{13}\text{C}_{\text{Suc}}$ for each organ and had similar organ-specific ^{13}C -enrichment as $\delta^{13}\text{C}_{\text{Suc}}$, with lowest $\delta^{13}\text{C}_{\text{Glc}}$ in needles and highest in roots (Table 1 and Figure 5). In roots, $\delta^{13}\text{C}_{\text{Glc}} > \delta^{13}\text{C}_{\text{Suc}}$ [$1.2 \pm 0.6\text{‰}$, $t(52) = 3.526$, $p < 0.001$]. In phloem, $\delta^{13}\text{C}_{\text{Glc}} > \delta^{13}\text{C}_{\text{Suc}}$, when considering the standard deviations ($0.8 \pm 0.6\text{‰}$, $n = 13$). However, it should be noted that the replication

was relatively low for phloem $\delta^{13}\text{C}_{\text{Glc}}$ series because the abundance of glucose was often low in phloem (Table 2 and Figure 5). In needles, $\delta^{13}\text{C}_{\text{Glc}} \approx \delta^{13}\text{C}_{\text{Suc}}$ ($0.4 \pm 0.8\text{‰}$) (Table 2).

The $\delta^{13}\text{C}_{\text{WSC}}$ series correlated well with $\delta^{13}\text{C}_{\text{Suc}}$ and/or $\delta^{13}\text{C}_{\text{Glc}}$ series for all organs (Table 1) but had relatively low day-to-day variability. The latter was due to the presence of pinitol, whose

TABLE 2 The abundance (%) of different carbohydrate compounds in the total water-soluble carbohydrate (WSC) fraction in different organs of the *Pinus sylvestris* saplings, together with their average $\delta^{13}\text{C}$ values.

	Abundance of WSCs (%)				$\delta^{13}\text{C}$ (‰)				
	0N	1N	Phloem	Roots	0N	1N	Needles (0N + 1N)	Phloem	Roots
Sucrose	26 ± 11	17 ± 9	86 ± 27	31 ± 11	-29.5 ± 1.3	-28.3 ± 1.5	-29.0 ± 1.3	-28.3 ± 1.2	-27.3 ± 1.0
Glucose	24 ± 8	29 ± 7	16 ± 7	28 ± 8	-28.8 ± 1.2	-28.0 ± 0.9		-27.3 ± 1.1	-26.2 ± 1.1
Pinitol	62 ± 6	50 ± 10	20 ± 5	29 ± 5	-30.3 ± 0.5	-32.0 ± 0.2		-31.1 ± 0.4	-31.2 ± 0.3
WSC					-29.3 ± 0.8	-29.1 ± 0.7	-29.2 ± 0.7	-29.1 ± 0.7	-27.8 ± 0.5

Note: The studied organs included current-year needles (0 N), one-year-old needles (1 N), phloem and roots. The needle (0 N + 1 N) $\delta^{13}\text{C}$ value for sucrose and WSCs represents a mass balance calculation, based on the 1.5 times higher content of sucrose in 0 N than 1 N (see also Figure 6 for the correspondingly lower enzyme activity in 1 N). For glucose and pinitol, the needle (0 N + 1 N) $\delta^{13}\text{C}$ value was not calculated, because these compounds are not transported down-stem from leaves and the values are hence irrelevant for the study.

carbon isotope composition ($\delta^{13}\text{C}_{\text{Pinitol}}$) did not show much temporal variability (Table 2 and Figure 5), and did not correlate with $\delta^{13}\text{C}_{\text{Suc}}$ or $\delta^{13}\text{C}_{\text{Glc}}$ for any organ ($p > 0.05$). Pinitol was ^{13}C -depleted relative to sugars, and its abundance and $\delta^{13}\text{C}$ value were organ specific (Table 2 and Figure 5). There was no offset between $\delta^{13}\text{C}_{\text{WSC}_0\text{N}}$ and $\delta^{13}\text{C}_{\text{WSC}_1\text{N}}$ or between $\delta^{13}\text{C}_{\text{WSC}_\text{Needle}}$ and $\delta^{13}\text{C}_{\text{WSC}_\text{Phloem}}$, only roots showed ^{13}C -enrichment (Figure 5).

$\delta^{13}\text{C}_{\text{P}_\text{calc}}$ data ($-29.6 \pm 1.5\text{‰}$) did not significantly differ from $\delta^{13}\text{C}_{\text{Suc}_1\text{N}}$ ($-28.4 \pm 2.0\text{‰}$, $p > 0.05$), but the daily average $\delta^{13}\text{C}_{\text{P}_\text{calc}}$ values had 2.5 ± 2.3 times higher standard deviations. $\delta^{13}\text{C}_{\text{P}_\text{calc}}$ had significant correlations with $\delta^{13}\text{C}_{\text{Suc}}$, $\delta^{13}\text{C}_{\text{Glc}}$ and $\delta^{13}\text{C}_{\text{WSC}}$ in the studied organs (Table 1).

Statistically significant environmental (RH) and physiological signals (g_s , A, c_i and iWUE) were observed for $\delta^{13}\text{C}_{\text{Suc}_0\text{N}}$, $\delta^{13}\text{C}_{\text{Suc}_\text{Phloem}}$ and $\delta^{13}\text{C}_{\text{Suc}_\text{Root}}$, but not of $\delta^{13}\text{C}_{\text{Suc}_1\text{N}}$, despite the significant correlation between $\delta^{13}\text{C}_{\text{Suc}_1\text{N}}$ and $\delta^{13}\text{C}_{\text{Suc}_0\text{N}}$ (Table 1). For $\delta^{13}\text{C}_{\text{Glc}}$ and $\delta^{13}\text{C}_{\text{WSC}}$, also the 1 N series correlated. When July 16, the sampling day with the VPD maxima (Figure 4), was excluded from correlation analysis, correlations with $\delta^{13}\text{C}_{\text{P}_\text{calc}}$ (Figure 5a) and iWUE were generally improved (Table 1). On this day, the typical negative correlation between c_i and the measured $\delta^{13}\text{C}$ series was inverted (Figure 5).

3.3 | Starch $\delta^{13}\text{C}$ and concentration in 1 N

Needle starch $\delta^{13}\text{C}$ ($\delta^{13}\text{C}_{\text{Starch}_1\text{N}}$) was invariable during the experiment, unlike needle sugars, and on average more ^{13}C -depleted (no blank correction: $-28.9 \pm 0.4\text{‰}$, corrected: $-30.3 \pm 0.5\text{‰}$) than $\delta^{13}\text{C}_{\text{Suc}_1\text{N}}$ ($-28.2 \pm 2.0\text{‰}$) and $\delta^{13}\text{C}_{\text{Glc}_1\text{N}}$ ($-28.0 \pm 1.4\text{‰}$) but similar to $\delta^{13}\text{C}_{\text{WSC}_1\text{N}}$ ($-29.1 \pm 0.7\text{‰}$) (Figures 3 and 5). $\delta^{13}\text{C}_{\text{Starch}_1\text{N}}$ was significantly affected by blank correction ($p < 0.001$; $\delta^{13}\text{C}_{\text{Blank}}$: -27.6 ± 0.6 , $n = 26$), caused by low starch content in analysed samples. The correlation of starch concentration with blank corrected $\delta^{13}\text{C}_{\text{Starch}_1\text{N}}$ ($r = 0.73$, $p < 0.05$), but not with uncorrected $\delta^{13}\text{C}_{\text{Starch}_1\text{N}}$, can be associated with the correction procedure and suggests overcorrection of the $\delta^{13}\text{C}_{\text{Starch}_1\text{N}}$ data. Starch concentration was stable during the first 5 weeks of experiment, but then

significantly declined ($p < 0.01$) on July 16, coinciding with the VPD maxima, and significantly increased ($p < 0.01$) week later.

3.4 | Enzymatic activity of needles

The activity of the enzymes synthesizing sucrose or degrading it to glucose and fructose in needles was on average 3.1 times higher in 0 N than 1 N (Figure 6). The enzyme activities did not correlate with $\delta^{13}\text{C}$ or concentration series of the sugars or with the leaf gas exchange variables. Similarly, there were no significant correlations between the relative activities of the sucrose degrading enzymes, calculated as the difference between the activity of INV_{acid} and $\text{SuSy}_{\text{degradation}}$, and the offset between $\delta^{13}\text{C}_{\text{Suc}}$ and $\delta^{13}\text{C}_{\text{Glc}}$.

3.5 | Intra-annual tree-ring $\delta^{13}\text{C}$ variability

In some of the specimens, the studied annual ring of 2018 contained compression wood, a type of reaction wood that is found in leaning conifer stems for tree support (Timell, 1986). These sections were used together with normal density wood for $\delta^{13}\text{C}$ analysis, because their width enabled relatively high spatial resolution $\delta^{13}\text{C}$ profiling, and since no ^{13}C -fractionation was observed in connection to the formation of compression wood (Supporting Information: Figure S3 and Method S3), in accordance with Walia et al. (2010) and Janecka et al. (2020).

$\delta^{13}\text{C}_{\text{Ring}_\text{RE}}$ profiles had a general increasing trend until June 5, followed by a decline that reached a distinct minimum by July 2 (Figure 2). This time period included the transition from EW to LW in tree-ring composition. For the remaining period of the experiment, $\delta^{13}\text{C}$ values had a general increasing trend. The overall low frequency trend in $\delta^{13}\text{C}_{\text{Ring}_\text{RE}}$ profiles was similar to that observed for phloem $\delta^{13}\text{C}_{\text{Suc}}$ and $\delta^{13}\text{C}_{\text{Glc}}$ series, which were fitted in Figure 2 using the common sampling days for phloem and tree-rings (Supporting Information: Method S1) The average $\delta^{13}\text{C}$ value of the July 2 and July 30 tree-ring series was then calculated from Figure 2 for each phloem sampling day (Table 3). The average of all $\delta^{13}\text{C}$ datapoints on

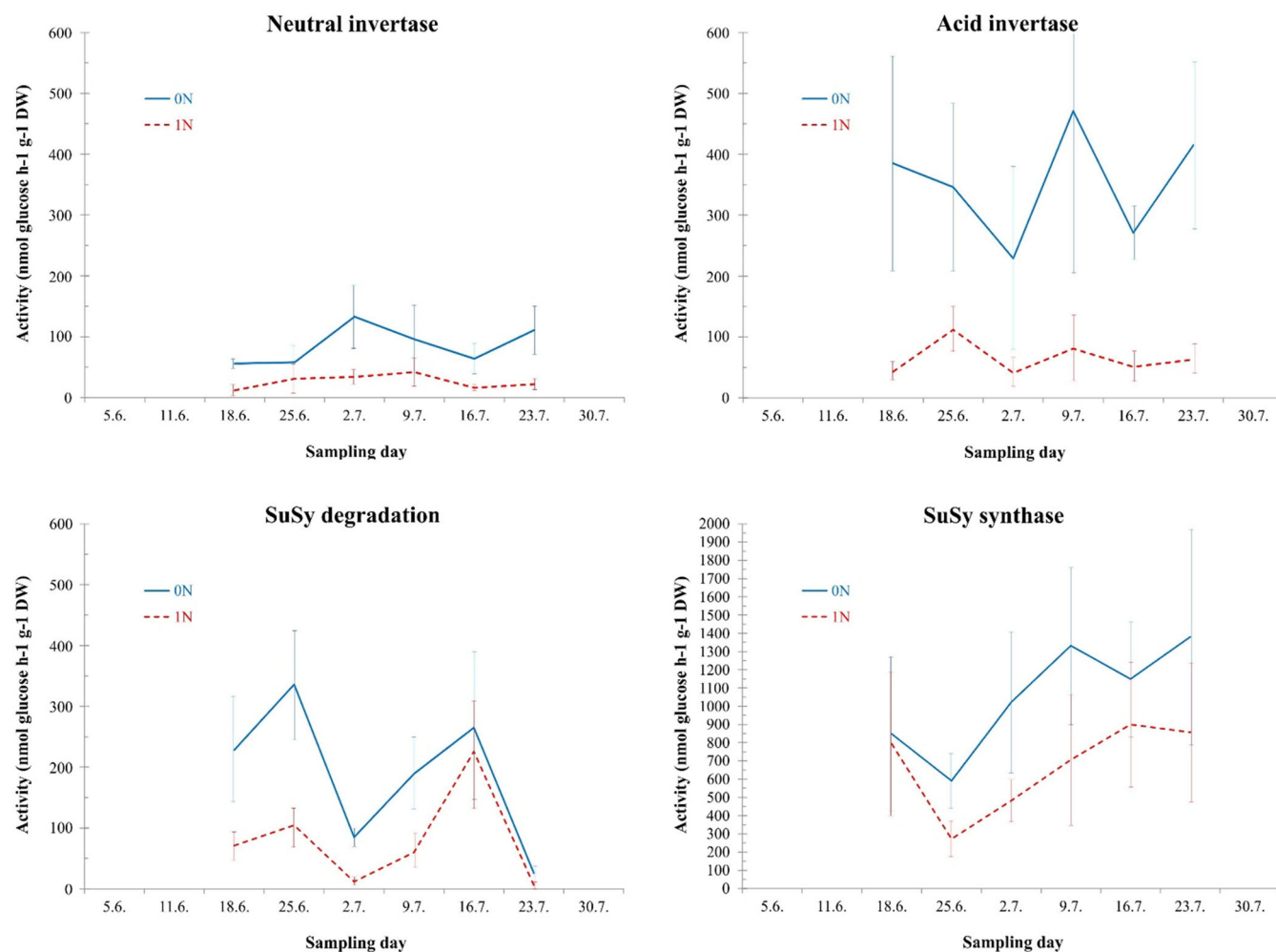


FIGURE 6 Activity of enzymes involved in sucrose formation and breakdown in current-year (0 N) and 1-year-old (1 N) needles of *Pinus sylvestris* saplings. Each data point represents the average of four trees and the error bars its standard deviations (clones A, B, C and D). The temporal changes had clear similarities for the two needle generations, although the correlations were not statistically significant for these short datasets. The activities were higher in 0 N than 1 N: on average 3.3 times for neutral invertase, 5.4 times for acid invertase, 2.0 for sucrose-degrading sucrose synthase (SuSy) and 1.6 times for sucrose-synthetizing SuSy.

TABLE 3 The average $\delta^{13}\text{C}$ value of the resin extracted tree-rings of *Pinus sylvestris* saplings for each phloem sampling day, as calculated from Figure 2.

June 5	June 11	June 18	June 25	July 2	July 9	July 16	July 23	July 30
$-26.6 \pm 0.7\%$	$-27.4 \pm 1.0\%$	$-28.7 \pm 1.1\%$	$-30.0 \pm 0.8\%$	$-29.8 \pm 0.6\%$	$-29.2 \pm 0.6\%$	$-28.7 \pm 1.0\%$	$-28.7 \pm 0.9\%$	$-28.5 \pm 0.8\%$

EW was $-27.2 \pm 0.6\%$, when calculated for each clone of July 2 and July 30 (Figure 2). The average of LW was $-29.5 \pm 0.45\%$ for July 30 samples. When more than one segment had been measured for a clone, the average $\delta^{13}\text{C}$ of a clone was first calculated before the calculation of the EW and LW average.

The $\delta^{13}\text{C}$ value of resin extracted EW and LW dissections of July 30 samples from EA-IRMS analysis were $-27.9 \pm 0.9\%$ and $-29.9 \pm 0.7\%$, respectively, agreeing well with the calculated average $\delta^{13}\text{C}$ values from LA-IRMS analysis. Cellulose extracted from the same sections had $\delta^{13}\text{C}$ values $1.2 \pm 0.4\%$ higher in comparison to resin extracted wood.

4 | DISCUSSION

4.1 | Environmental and physiological signal in $\delta^{13}\text{C}_{\text{Suc}}$, $\delta^{13}\text{C}_{\text{Glc}}$ and $\delta^{13}\text{C}_{\text{WSC}}$

4.1.1 | Leaves

The observation that the temporal changes in leaf $\delta^{13}\text{C}_{\text{Suc}}$ and $\delta^{13}\text{C}_{\text{Glc}}$ recorded RH and g_s , and were overall predicted by $\delta^{13}\text{C}_{\text{P_calc}}$ (Table 1 and Figure 5) suggests a generally negligible role of old reserve use for these carbon pools. This is supported by the

invariable and low starch $\delta^{13}\text{C}$ in 1N (Figure 3). The environmentally driven $\delta^{13}\text{C}$ of leaf sugars is in accordance with studies on mature *L. gmelinii* (Rinne, Saurer, Kirilyanov, Bryukhanova, et al., 2015), *Larix decidua* (Sidorova et al., 2019) and *P. sylvestris* (Tang, Schiestl-Aalto, Lehmann, et al., 2022), where high resolution sampling during a growing season showed a significant climatic signal in $\delta^{13}\text{C}_{\text{Suc}}$ and $\delta^{13}\text{C}_{\text{Glc}}$ values with little or no sign of reserve use. In contrast, the climatic and physiological signal of $\delta^{13}\text{C}$ from bulk leaf matter may be reduced or distorted, due to the high proportion of other compounds, such as pinitol (Table 2) or starch (Figure 3), with slow turnover rate and different metabolic history (Leppä et al., 2022; Rinne, Saurer, Kirilyanov, Bryukhanova, et al., 2015; Streit et al., 2013). Similarly, Bögelein et al. (2019) reported absence of diel variation in leaf and twig phloem $\delta^{13}\text{C}_{\text{WSC}}$ of Douglas fir, which they assigned to large abundance of pinitol. However, the present study, which for the first time compared temporal changes in $\delta^{13}\text{C}_{\text{WSC}}$ with those in $\delta^{13}\text{C}_{\text{Suc}}$ and $\delta^{13}\text{C}_{\text{Glc}}$, suggests that $\delta^{13}\text{C}_{\text{WSC}}$ can be an equally strong proxy record of intra-seasonal environmental variability and tree physiology as $\delta^{13}\text{C}_\text{P}$ (Table 1), although with isotopic offset and smaller amplitude of variation due to the presence of pinitol (Table 2 and Figure 5). This finding is significant for future studies, considering the rarity of HPLC-IRMS instruments for CSIA. Yet, the synchrony between $\delta^{13}\text{C}_{\text{WSC}}$ and $\delta^{13}\text{C}_{\text{Suc}}$ may not be present for trees exposed to more significant environmental stress than encountered in this study, considering that an increase in synthesis of pinitol, for example due to drought (Ford, 1984; Rinne, Saurer, Kirilyanov, Bryukhanova, et al., 2015), would cause a decline in $\delta^{13}\text{C}_{\text{WSC}}$.

The unconventional increase (vs. decrease) in leaf $\delta^{13}\text{C}$ series with increase in c_i observed in the July 16 sampling (Figure 5, c_i with reversed y-axis scale), the sampling day with the VPD maxima and the A minima (Figure 4), may be explained by utilization of carbohydrate reserves (Jäggi et al., 2002), as suggested by the significant decline in 1N starch concentration on July 16 ($p > 0.01$, Figure 3). However, the increase in $\delta^{13}\text{C}_{\text{Glc}}$ on July 16 is inconsistent with $\delta^{13}\text{C}_{\text{Starch}}$ values, which may indicate transport of sucrose from down-stem, such as twigs, to 1N at this time. Alternative, or complimentary mechanism, may be isotopic discrimination caused by mesophyll conductance, the diffusion of CO_2 from the substomatal cavity to the carboxylation sites (Flexas et al., 2008). Mesophyll conductance has been shown to decline in response to water stress, leading to reduced ^{13}C -discrimination during assimilation (Schiestl-Aalto et al., 2021).

4.1.2 | Modification of $\delta^{13}\text{C}_{\text{Suc}}$, $\delta^{13}\text{C}_{\text{Glc}}$ and $\delta^{13}\text{C}_{\text{WSC}}$ signal from needles to sink organs

This first simultaneous comparison of $\delta^{13}\text{C}$ data for individual sugars, together with WSCs, in leaves, phloem and roots at intra-seasonal resolution allows us to explain some of the controversy in the literature concerning post-photosynthetic fractionation processes. In the following, we will scrutinize the main possible mechanisms reported in the literature in light of this data set. Although results from sapling studies can be an oversimplification for mature trees

growing in the field (Johnson & Ball, 1996), for example due to their smaller reserve pool size, it is this simplified experimental design that improves our ability to identify the main individual isotope fractionation processes.

The temporal $\delta^{13}\text{C}$ changes in needles were well preserved in sink organ $\delta^{13}\text{C}_{\text{Suc}}$, $\delta^{13}\text{C}_{\text{Glc}}$ and $\delta^{13}\text{C}_{\text{WSC}}$. However, sucrose became progressively ^{13}C -enriched from needles to phloem and roots, consistently throughout the experiment (Figures 5 and 7). The ^{13}C -enrichment of sink organs relative to leaves has been commonly reported and the associated mechanisms widely debated (Cernusak et al., 2009; Gessler, Brandes, et al., 2009). Conventionally a bulk matter, such as WSCs or total organic matter, has been used for the $\delta^{13}\text{C}$ analysis, which may complicate the interpretations on post-photosynthetic isotope fractionations, considering that each compound within the mixture can differ in its $\delta^{13}\text{C}$ value due to their metabolic formation pathways having different C isotope effects (Tcherkez et al., 2011). Indeed, this was seen for needle $\delta^{13}\text{C}_{\text{WSC}}$ (Figure 5), which did not record the $\sim 1.2\text{‰}$ difference between sucrose in 1N and sucrose in 0N, because the offset was balanced by the $\sim 1.7\text{‰}$ lower $\delta^{13}\text{C}_{\text{Pinitol}_{1N}}$ compared to $\delta^{13}\text{C}_{\text{Pinitol}_{0N}}$ (Table 2). Similarly, if only $\delta^{13}\text{C}_{\text{WSC}}$ had been analysed in the present study, it would not have been possible to observe the ^{13}C -enrichment of needle sugars along their transport route in phloem (Figure 7). This is because $\delta^{13}\text{C}$ value and abundance of pinitol, constituent of WSCs, varied greatly between the organs (Table 2).

CSIA studies on larch in Siberia (Rinne, Saurer, Kirilyanov, Bryukhanova, et al., 2015; Rinne, Saurer, Kirilyanov, Loader, et al., 2015) proposed that the generally reported ^{13}C -enrichment of sink organs relative to leaves is in large parts caused by the high abundance of ^{13}C -depleted pinitol in leaves and the INV_{acid} induced ^{13}C -enrichment of leaf sucrose relative to hexoses (Gilbert et al., 2011; Mauve et al., 2009). However, the role of INV_{acid} associated fractionation is inconsistent between the published studies: the level of ^{13}C -enrichment of sucrose over hexose is

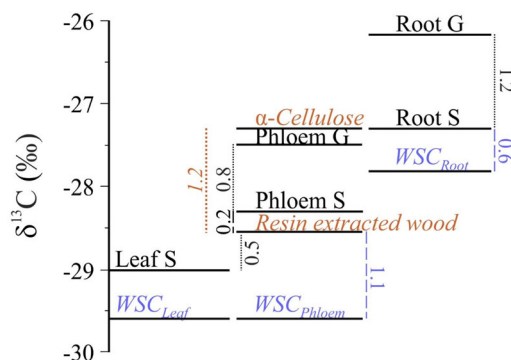


FIGURE 7 Average $\delta^{13}\text{C}$ values and isotopic offsets (vertical numbers) between sucrose (S), glucose (G), water-soluble carbohydrates (WSC) and tree rings of *Pinus sylvestris* saplings. $\delta^{13}\text{C}$ of S, G and WSC were measured for needles, phloem and roots (Figure 5). S and G were measured with HPLC-IRMS, WSC and wood α -cellulose with EA-IRMS, and resin extracted wood using laser ablation (Figure 2).

variable (e.g., Sidorova et al., 2018), even within a growing season (Rinne, Saurer, Kirilyanov, Bryukhanova, et al., 2015), or not detectable (the present study). This inconsistency may indicate species-specific differences (Dominguez & Niittylä, 2021), tree health status (Sidorova et al., 2018) or differences in the activity level of INV_{acid} (Rinne, Saurer, Kirilyanov, Loader, et al. 2015). The present study provided the first opportunity to examine, if changes in the relative activity of INV_{acid} and $\text{SuSy}_{\text{degradation}}$ in sucrose breakdown to hexoses can be used to explain temporal changes in the isotopic offset between sucrose and hexoses in leaves (Rinne, Saurer, Kirilyanov, Loader, et al., 2015), considering that no isotope fractionation is involved with activity of $\text{SuSy}_{\text{degradation}}$ (Gilbert et al., 2012). However, the lack of a significant correlation between the enzyme activities and $\delta^{13}\text{C}$ values of the sugars indicates that the processes leading to a given isotopic offset is more complex and will be discussed in detail below.

The ^{13}C -enrichment of leaf sucrose relative to leaf WSCs was not the only factor contributing to the ^{13}C -enrichment of sink organs relative to leaf WSCs in this study. The comparison of $\delta^{13}\text{C}_{\text{Suc}}$ of the studied organs demonstrates that during down-stem transport of sucrose from leaves to roots, its carbon isotope composition has been progressively altered by one or several fractionating processes (Figure 5). Since needle $\delta^{13}\text{C}_{\text{Suc}}$ recorded environmental change (Section 4.1.1) and the temporal variability in this series was not dampened but instead preserved in phloem and root $\delta^{13}\text{C}_{\text{Suc}}$ series (Figure 5), it seems unlikely that reserve use, such as starch pools of phloem parenchyma, or mixing of sugar pools of different age (Brandes et al., 2006) could explain the isotopic offsets between the three organs. Further, ^{13}C -enrichment of phloem $\delta^{13}\text{C}_{\text{Suc}}$ relative to needle $\delta^{13}\text{C}_{\text{Suc}}$ cannot be ascribed to remobilization of transitory starch during the night (Gessler & Ferrio, 2022), because needle starch reserves (uncorrected: $-28.9 \pm 0.1\%$, blank corrected: $-30.3 \pm 0.5\%$) were overall not ^{13}C -enriched compared to needle sucrose ($-28.3 \pm 1.5\%$) (Figure 3). The direction of the observed isotopic offset between starch and sugars is not in accordance with the general assumption about the relative ^{13}C -enrichment of starch over sucrose in leaves due to the aldolase reaction (Gleixner & Schmidt, 1997), but is in agreement with Lehmann et al. (2019), who did not detect an impact of the aldolase reaction on WSC $\delta^{13}\text{C}$ when utilizing mutants of four nontree C_3 species that lacked the enzyme phosphoglucomutase needed for starch production. These are cautionary findings for studies that link increases in $\delta^{13}\text{C}$ of, for example, photosynthates or tree-rings with reserve use without measuring starch $\delta^{13}\text{C}$. Furthermore, the ^{13}C -enrichment of phloem $\delta^{13}\text{C}_{\text{Suc}}$ relative to leaves should not be due to a higher proportion of sucrose from sunlit needles than that from sampled needles (Bögelein et al., 2019). This is because the trees were 1.4 m tall and their canopy evenly exposed to light, hence the sampled needles can be considered to be representative of the entire canopy (see Section 2.2). Also invertase activity in phloem, which was hypothesized in Mauve et al. (2009) to explain ^{13}C -enrichment of sucrose in sink organs relative to leaves, cannot fully explain our observations (Figure 5). This is because there is no primary isotope effect on

glucose during invertase catalysis (Mauve et al., 2009) and, hence, the enzyme activity cannot explain the observed ^{13}C -enrichment of glucose relative to sucrose in phloem and roots.

In contrast, the progressive ^{13}C -enrichment of sucrose along the pathway from leaves to phloem and roots, and the ^{13}C -enrichment of glucose relative to sucrose in sink organs, could be explained by fractionations in primary carbon metabolism [respiratory decarboxylations, pentose phosphate pathway (Bathellier et al., 2008) and phosphoenolpyruvatecarboxylase (PEPC) (Gessler, Tcherkez, et al., 2009)], leading to ^{13}C -enrichment of the remaining substrate (Cernusak et al., 2009; Ghashghaie et al., 2003; Gleixner et al., 1998). The impact of sink organ catabolism on $\delta^{13}\text{C}_{\text{Suc}}$ has been previously reported also for potato, where the 2‰ increase in tuber $\delta^{13}\text{C}_{\text{Suc}}$ over sprout or leaf sucrose was explained by this process (Gleixner et al., 1998; Maunoury-Danger et al., 2009). In the present study, the increase in $\delta^{13}\text{C}_{\text{Suc}}$ was 0.7‰ from leaves to phloem (Figure 5) and a further 1.0‰ increase from phloem to roots (Figures 5 and 7). Although our results are consistent with fractionation reactions associated with CO_2 production being the main cause of observed ^{13}C -enrichment in sink organ sucrose and glucose, other underlying processes may have contributed to the $\delta^{13}\text{C}_{\text{Suc}}$ offsets.

The exclusion of 2-year-old needles from the present study probably overestimated the impact of phloem CO_2 efflux on $\delta^{13}\text{C}_{\text{Suc}}$, considering that this needle generation likely had needle $\delta^{13}\text{C}_{\text{Suc}}$ similar to that in 1 N, in contrast with the metabolically active 0 N, which had relatively lower $\delta^{13}\text{C}_{\text{Suc}}$ values (Figures 5 and 6). However, this impact was likely small, because 0 and 1 N are the dominant needle generations in *P. sylvestris* (80% of all needles in Kurkela et al., 2009) and because there is a major decline in physiological activity of conifer needles with age (Drenkhan et al., 2006; Robakowski & Bielinis, 2017). In the present study, the more significant role of 0 N relative to 1 N in sugar dynamics was suggested by the 1.5 times higher sucrose content in 0 N and by the 3.1 times higher activity of the studied enzymes responsible for sucrose synthesis and breakdown in 0 N (Figure 6).

The fact that $\delta^{13}\text{C}_{\text{Glc}}$ was higher than $\delta^{13}\text{C}_{\text{Suc}}$ in sink organs (Figure 5), which was statistically significant for roots and within standard deviations for phloem, may also be explained by respiration, considering that glucose is the substrate for glycolysis. The relative ^{13}C -enrichment in glucose (compared to sucrose) in sink organs could come from glucose 6-phosphate consumption by catabolism, following glucose production by enzymatic sucrose cleavage. The impact of carbon loss by CO_2 formation on $\delta^{13}\text{C}_{\text{Glc}}$ can also explain why glucose was generally more ^{13}C -enriched than sucrose in sink organs but not in needles: whereas in sink organs the above discussed pentose phosphate pathway causes dark respired CO_2 to be ^{13}C -depleted relative to its substrate, in leaves the produced CO_2 is assumed to be ^{13}C -enriched (Bathellier et al., 2017; Ghashghaie et al., 2003). Since glucose can be used by respiration, and that stem and root $\delta^{13}\text{C}_{\text{Glc}}$ recorded the environmentally driven (Table 1) changes in leaf $\delta^{13}\text{C}_{\text{Suc}}$ (Figure 5), it is possible that the $\delta^{13}\text{C}$ pattern in respired CO_2 also followed fluctuations in photosynthetic ^{13}C -discrimination (Gessler et al., 2007).

Summarizing, our findings provide the missing evidence for earlier studies reporting sink organ ^{13}C -enrichment (Wingate et al., 2010) and could explain the observed correlations between sink organ respiration and environmental drivers (Barbour et al., 2005; Ekblad & Högberg, 2001). Future studies should, however, ascertain the role respiration on $\delta^{13}\text{C}$ of sink organ substrates with simultaneous measurements of $\delta^{13}\text{C}$ of respired CO_2 (Ghashghaie et al., 2003; Tcherkez et al., 2003).

4.2 | Intra-annual tree-ring $\delta^{13}\text{C}$ signal

4.2.1 | Isotopic offset between leaf sugars and tree-rings

Considering that only low-frequency trends (from 2 to 3 weeks) in climate and $\delta^{13}\text{C}_{\text{Suc}}$ can be preserved in tree-rings due to the development period of a xylem cell (Gessler, Brandes, et al., 2009; Pérez-de-Lis et al., 2022), the modification of $\delta^{13}\text{C}$ signal from needles to tree-rings appears to have been relatively simple. Both temporal changes and absolute values in $\delta^{13}\text{C}_{\text{Ring_RE}}$ series can be explained by $\delta^{13}\text{C}$ of phloem sugars, which recorded ambient environmental conditions from leaf photosynthesis but with a systematic shift in isotope composition by fractionating reactions contributing to phloem CO_2 efflux formation (Section 4.1.2). Our results indicate that the $\delta^{13}\text{C}_{\text{Glc}}$ of the pine saplings closely matched the $\delta^{13}\text{C}$ of cellulose (formed of glucose units), because the offset between resin extracted wood and glucose ($1.0 \pm 1.0\%$, Figure 7) was very similar to the offset between resin extracted wood and cellulose ($1.2 \pm 0.4\%$, Figure 7). Therefore, there was no evidence of the postulated isotope fractionation occurring during xylem cell formation ($\delta^{13}\text{C}_{\text{Glc}} \approx \delta^{13}\text{C}_{\text{Ring_Cellulose}}$) due to, for example, activity of the fractionating INV_{acid} (e.g., Panek & Waring, 1997; Rinne, Saurer, Kirilyanov, Loader, et al., 2015; Terwilliger et al., 2001). This finding suggests that $\text{SuSy}_{\text{degradation}}$, the non-fractionating enzyme, is responsible for providing substrate for the cellulose synthase complex, in line with Stein and Granot (2019). Evidence of ^{13}C -fractionating process during xylem formation are contradictory: none were found in *Eucalyptus globulus* between phloem sap and newly developing xylem tissue (Cernusak et al., 2005), but wholewood of *Pinus halepensis* was 1.4% ^{13}C -enriched compared to phloem sap (Gessler, Brandes, et al., 2009). We propose that such contradictive outcomes can be expected, when conducting $\delta^{13}\text{C}$ analysis on a bulk matter of phloem, because: (i) phloem sap contains sugar alcohols and/or raffinose with a distinctive $\delta^{13}\text{C}$ value (Bögelein et al., 2019; Merchant et al., 2010; Rinne, Saurer, Kirilyanov, Bryukhanova, et al., 2015), and the relative proportion of sucrose in phloem sap vary between sites and species, with for example, 80% for *E. globulus* in Australia (Merchant et al., 2010), 62% for *Pinus pinaster* in France (Devaux et al., 2009) and 50% for *Citrus sinensis* in another greenhouse experiment (Hijaz & Killiny, 2014); (ii) sucrose is degraded to hexoses for sink organ formation, with a systematic offset between sucrose and hexoses (Figure 5), probably due to fractionations in hexose metabolism (Section 4.1.2). This results in an apparent

fractionation between phloem sucrose and wood cellulose even if enzymatic processes responsible for cellulose formation are non-fractionating. Thus, the analysis of phloem sap comes with uncertainties that do not allow exact estimation of isotope fractionation processes. This is clearly illustrated in Figure 7, where the isotopic offsets between $\delta^{13}\text{C}_{\text{Ring}}$ and $\delta^{13}\text{C}_{\text{WSC}}$ in the analysed organs are very deviant from those between $\delta^{13}\text{C}_{\text{Ring}}$ and $\delta^{13}\text{C}_{\text{Suc}}$ or $\delta^{13}\text{C}_{\text{Glc}}$. Consequently, without CSIA, it would not have been possible to, for example, detect the role of $\text{SuSy}_{\text{degradation}}$ in cellulose formation or the postulated impact of carbon loss in sink organs by CO_2 formation on $\delta^{13}\text{C}_{\text{Ring}}$.

The observed 0.5% ^{13}C -enrichment of $\delta^{13}\text{C}_{\text{Ring_RE}}$ relative to $\delta^{13}\text{C}_{\text{Suc_Needle}}$ is relevant for environmental and tree physiological reconstructions that are based on the absolute tree-ring $\delta^{13}\text{C}$ values, such as iWUE (Figure 7). Further, it is important to determine how this isotopic offset may vary between sites and species. The two other publications that have combined CSIA of leaf photosynthates with $\delta^{13}\text{C}$ profiling of tree-rings reported 1.0 and 0.9% higher values for $\delta^{13}\text{C}_{\text{Ring_RE}}$ of mature *L. gmelinii* in central Siberia (Rinne, Saurer, Kirilyanov, Loader, et al., 2015) and mature *P. sylvestris* in southern Finland (Tang et al., 2023), respectively. There are several factors to consider, when evaluating such offsets in $\delta^{13}\text{C}$ between studies. (i) There may be species- and site-specific differences in INV_{acid} -induced fractionation, as discussed in Section 4.1. By removing the impact of INV_{acid} on $\delta^{13}\text{C}_{\text{Suc_Needle}}$ in Rinne, Saurer, Kirilyanov, Loader, et al. (2015), the difference between $\delta^{13}\text{C}_{\text{Ring_RE}}$ and $\delta^{13}\text{C}_{\text{Suc_Needle}}$ is reduced to 0.4% , which is similar to our finding (Figure 7). (ii) The magnitude of CO_2 efflux associated isotope fractionation along the pathway from leaves to stem xylem could increase with tree height, potentially leading to a bigger isotopic offset between leaf sugars and tree-rings for mature trees, for example in Tang et al. (2023). (iii) When using mature trees for studying post-photosynthetic ^{13}C -fractionation, it can be challenging to obtain canopy-representative CSIA results, considering that $\delta^{13}\text{C}_{\text{P}}$ is dependent on the incident solar energy received by the leaves (Bögelein et al., 2019; Schleser, 1989). Whereas this could affect the results of Tang et al. (2023), where needles were collected from the upper part of a dense canopy, it probably did not impact the finding of Rinne, Saurer, Kirilyanov, Loader, et al. (2015), where the canopies were small and tree density low, providing more or less equal light levels for needles around the canopy. Our study thus shows that the estimation of absolute values of iWUE derived from $\delta^{13}\text{C}_{\text{Ring}}$ are still hampered by difficulties in our understanding of isotope fractionation processes between plant assimilate and ring material.

The measured ^{13}C -enrichment of resin extracted wood relative to cellulose by 1.2% (Figure 7) is smaller than the 1.8 and 2% reported for conifers *L. gmelinii* and *Pseudotsuga menziesii*, respectively (Livingston & Spittlehouse, 1996; Sidorova et al., 2010). However, our results may not be directly comparable to the previous findings due to differences in chemical extraction procedures of the analysed wood. The possible reasons are (i) the duration of resin extraction, which was shorter or not reported in the previous studies, and (ii) removal of hemicelluloses during α -cellulose extraction, considering that this step was not done in Livingston and Spittlehouse (1996) and Sidorova et al. (2010). Resins are up to

6‰ depleted relative to cellulose (Schmidt & Gleixner, 1998) and hemicelluloses isotopically differ from α -cellulose (Boettger et al., 2007), and, therefore, the presence of these substrates in Livingston and Spittlehouse (1996) and Sidorova et al. (2010) could explain the differences between our results. Another potential explanator is a difference in lignin to cellulose content ratio in the analysed samples, considering that lignin is relatively ^{13}C -depleted (Bowling et al., 2008) and its abundance is not constant between gymnosperms (Ana & Helena, 2017).

4.2.2 | Environmental signal in EW $\delta^{13}\text{C}$

There was no observable evidence for use of reserves for tree-ring growth under the studied conditions, characterized by relatively high ambient T and VPD levels, which sometimes limited gas exchange (Figure 4) and which are the likely reason for the narrow LW bands formed in 2018 (Zweifel et al., 2021). The low frequency trends and absolute values of the intra-annual $\delta^{13}\text{C}_{\text{Ring, RE}}$ series can be explained by the phloem sugar $\delta^{13}\text{C}$ values (Figure 2, section 4.3.1.1), which recorded changes in c_i and the subsequent post-photosynthetic isotope fractionations caused by CO_2 production (Section 4.1). For the EW section formed before June 5 (Figure 2), there is no sugar data available for a similar evaluation, however, the initial increase in EW $\delta^{13}\text{C}$ can be explained by the acclimation of the saplings to the warmer conditions in greenhouse after their transport from the field on May 17 ($T_{\text{diff}} = 7^\circ\text{C}$).

Hence, we propose/confirm, as hypothesized in Monson et al. (2018) and indicated in Tang et al. (2023), that it may not be necessary to discard the EW section of $\delta^{13}\text{C}$ chronologies for tree physiological and paleoenvironmental studies, when studying conifers, such as *Pinus* (this study) and *Larix* (Rinne, Saurer, Kirilyanov, Loader, et al., 2015), in boreal forests under non-stressed to mildly stressed conditions. Apart from providing valuable information about the processes occurring during the early part of the growing season, this outcome would also give further confidence for the interpretation of $\delta^{13}\text{C}$ chronologies constructed using the whole annual ring, for example, because of the presence of too narrow LW sections for manual dissection (Vitali et al., 2022).

5 | CONCLUSIONS

Our $\delta^{13}\text{C}$ data set, which combines compound-specific sugar data obtained from leaves, phloem and roots at weekly resolution with high spatial resolution tree-ring series of *P. sylvestris*, provided a close insight into the metabolic processes that occur and modify a $\delta^{13}\text{C}_\text{P}$ before the isotopic record is deposited in tree-rings. The observations indicated a relatively simple pattern, where the progressive ^{13}C -enrichment of $\delta^{13}\text{C}_\text{P}$ from needles via phloem to roots is perhaps explained by sink organ catabolic CO_2 loss (question 2 in Introduction). There was no evidence of phloem loading distorting the $\delta^{13}\text{C}_\text{P}$ signal (question 1). The observation of lower $\delta^{13}\text{C}_\text{P}$ relative to $\delta^{13}\text{C}_{\text{Ring, RE}}$ and $\delta^{13}\text{C}_{\text{Ring, Cellulose}}$ are important for studies using $\delta^{13}\text{C}_{\text{Ring}}$ for, for example, iWUE reconstructions (question 3). The significant

environmental signal recorded in $\delta^{13}\text{C}_\text{P}$ was preserved in intra-annual $\delta^{13}\text{C}_{\text{Ring}}$ at low frequency scale, demonstrating negligible role of reserve use for EW or LW formation for these saplings (question 2). This is promising also for studies aiming for high-resolution, seasonally resolved climate reconstructions, at least when using pine species in boreal regions. The comparison of intra-seasonal $\delta^{13}\text{C}_{\text{WSC}}$ and $\delta^{13}\text{C}_\text{P}$ signals in different organs demonstrated that a bulk organic matter is unreliable proxy record for studies of post-photosynthetic isotope fractionation, but that $\delta^{13}\text{C}_{\text{WSC}}$ may perform equally well as $\delta^{13}\text{C}$ of individual sugars for reconstructions of intra-seasonal environmental variability and tree physiology. The outcomes of this study have relevance for the utilization of tree-rings as a proxy of environmental change and for studies interested in $\delta^{13}\text{C}$ of sink organ respiration and its environmental drivers (Barbour et al., 2005; Ekblad & Höglberg, 2001).

ACKNOWLEDGEMENTS

We would like to thank Juhani Pyykkö, Iman Karmoun, Aino Seppänen, Kira Ryhti and Kaarina Pynnönen for their valuable fieldwork assistance, and Aino Seppänen, Fana Gizaw, Marine Manche for efforts in sample preparation. We are grateful to Manuela Oettli for the HPLC-IRMS analysis. We would like to thank the Associate Editor and three anonymous reviewers for constructive comments. This study was financially supported by the European Research Council (755865), Academy of Finland (295319, 323843) and Swiss National Science Foundation (179978, 207360).

DATA AVAILABILITY STATEMENT

The data that support the findings of this study are available from the corresponding author upon reasonable request.

ORCID

Katja T. Rinne-Garmston  <http://orcid.org/0000-0001-9793-2549>

Yu Tang  <http://orcid.org/0000-0002-2851-4762>

Matthias Saurer  <http://orcid.org/0000-0002-3954-3534>

Yann Salmon  <http://orcid.org/0000-0003-4433-4021>

REFERENCES

- Adams, M.A., Buckley, T.N. & Turnbull, T.L. (2020) Diminishing CO_2 -driven gains in water-use efficiency of global forests. *Nature Climate Change*, 10(5), 466–471.
- Ana, L. & Helena, P. (2017) Compositional variability of lignin in biomass. In: Matheus, P. (Ed.) *Lignin*. IntechOpen.
- Barbour, M.M., Hunt, J.E., Dungan, R.J., Turnbull, M.H., Brailsford, G.W., Farquhar, G.D. et al. (2005) Variation in the degree of coupling between $\delta^{13}\text{C}$ of phloem sap and ecosystem respiration in two mature *Nothofagus* forests. *New Phytologist*, 166, 497–512.
- Bathellier, C., Badeck, F.-W., Couzi, P., Harscoët, S., Mauve, C. & Ghashghaie, J. (2008) Divergence in $\delta^{13}\text{C}$ of dark respired CO_2 and bulk organic matter occurs during the transition between heterotrophy and autotrophy in *Phaseolus vulgaris* plants. *New Phytologist*, 177(2), 406–418.
- Bathellier, C., Badeck, F.-W. & Ghashghaie, J. (2017) Carbon isotope fractionation in plant respiration. In: Tcherkez, G. & Ghashghaie, J. (Eds.) *Plant respiration: metabolic fluxes and carbon balance*. Springer International Publishing, pp. 43–68.

- Boettger, T., Haupt, M., Knöller, K., Weise, S.M., Waterhouse, J.S., Rinne, K.T. et al. (2007) Wood cellulose preparation methods and mass spectrometric analyses of $\delta^{13}\text{C}$, $\delta^{18}\text{O}$, and nonexchangeable $\delta^2\text{H}$ values in cellulose, sugar, and starch: an interlaboratory comparison. *Analytical Chemistry*, 79(12), 4603–4312.
- Bögelein, R., Lehmann, M.M. & Thomas, F.M. (2019) Differences in carbon isotope leaf-to-phloem fractionation and mixing patterns along a vertical gradient in mature European beech and Douglas fir. *New Phytologist*, 222(4), 1803–1815.
- Bowling, D.R., Pataki, D.E. & Randerson, J.T. (2008) Carbon isotopes in terrestrial ecosystem pools and CO_2 fluxes. *New Phytologist*, 178, 24–40.
- Brandes, E., Kodama, N., Whittaker, K., Weston, C., Rennenberg, H., Keitel, C. et al. (2006) Short-term variation in the isotopic composition of organic matter allocated from the leaves to the stem of *Pinus sylvestris*: effects of photosynthetic and postphotosynthetic carbon isotope fractionation. *Global Change Biology*, 12(10), 1922–1939.
- Brüggemann, N., Gessler, A., Kayler, Z., Keel, S.G., Badeck, F., Barthel, M. et al. (2011) Carbon allocation and carbon isotope fluxes in the plant-soil-atmosphere continuum: a review. *Biogeosciences*, 8(11), 3457–3489.
- Cernusak, L.A., Farquhar, G.D. & Pate, J.S. (2005) Environmental and physiological controls over oxygen and carbon isotope composition of Tasmanian blue gum, *Eucalyptus globulus*. *Tree Physiology*, 25, 129–146.
- Cernusak, L.A., Tcherkez, G., Keitel, C., Cornwell, W.K., Santiago, L.S., Knohl, A. et al. (2009) Why are non-photosynthetic tissues generally ^{13}C enriched compared with leaves in C_3 plants? Review and synthesis of current hypotheses. *Functional Plant Biology*, 36(3), 199.
- Dennis, D.T. & Blakeley, S.D. (2000) *Carbohydrate metabolism. Biochemistry and molecular biology of plants*. American Society of Plant Physiologists.
- Devaux, M., Ghashghaie, J., Bert, D., Lambrot, C., Gessler, A., Bathellier, C. et al. (2009) Carbon stable isotope ratio of phloem sugars in mature pine trees throughout the growing season: comparison of two extraction methods. *Rapid Communications in Mass Spectrometry*, 23(16), 2511–2518.
- Dominguez, P.G. & Niittylä, T. (2021) Mobile forms of carbon in trees: metabolism and transport. *Tree Physiology*, 42(3), 458–487.
- Drenkhan, R., Kurkela, T. & Hanso, M. (2006) The relationship between the needle age and the growth rate in Scots pine (*Pinus sylvestris*): a retrospective analysis by needle trace method (NTM). *European Journal of Forest Research*, 125(4), 397–405.
- Ekblad, A. & Höglberg, P. (2001) Natural abundance of ^{13}C in CO_2 respired from forest soils reveals speed of link between tree photosynthesis and root respiration. *Oecologia*, 127, 305–308.
- Etien, N., Daux, V., Masson-Delmotte, V., Mestre, O., Stievenard, M., Guillemin, M.T. et al. (2009) Summer maximum temperature in northern France over the past century: instrumental data versus multiple proxies (tree-ring isotopes, grape harvest dates and forest fires). *Climatic Change*, 94(3), 429–456.
- Farquhar, G., O'Leary, M. & Berry, J. (1982) On the relationship between carbon isotope discrimination and the intercellular carbon dioxide concentration in leaves. *Functional Plant Biology*, 9, 121–137.
- Farquhar, G.D., Ehleringer, J.R. & Hubick, K.T. (1989) Carbon isotope discrimination and photosynthesis. *Annual Review of Plant Physiology and Plant Molecular Biology*, 40, 503–537.
- Flexas, J., Ribas-Carbó, M., Diaz-Espejo, A., Galmés, J. & Medrano, H. (2008) Mesophyll conductance to CO_2 : current knowledge and future prospects. *Plant, Cell & Environment*, 31(5), 602–621.
- Fonti, M., Vaganov, E., Wirth, C., Shashkin, A., Astrakhantseva, N. & Schulze, D. (2018) Age-effect on intra-annual $\delta^{13}\text{C}$ -variability within Scots pine tree-rings from central Siberia. *Forests*, 9, 364.
- Ford, C.W. (1984) Accumulation of low molecular weight solutes in waterstressed tropical legumes. *Phytochemistry*, 23, 1007–1015.
- Galiano, L., Timofeeva, G., Saurer, M., Siegwolf, R., Martínez-Vilalta, J., Hommel, R. et al. (2017) The fate of recently fixed carbon after drought release: towards unravelling C storage regulation in *Tilia platyphyllos* and *Pinus sylvestris*. *Plant, Cell & Environment*, 40(9), 1711–1724.
- Gessler, A., Brandes, E., Buchmann, N., Helle, G., Rennenberg, H. & Barnard, R.L. (2009) Tracing carbon and oxygen isotope signals from newly assimilated sugars in the leaves to the tree-ring archive. *Plant, Cell and Environment*, 32, 780–795.
- Gessler, A., Ferrio, J.P., Hommel, R., Treydte, K., Werner, R.A. & Monson, R.K. (2014) Stable isotopes in tree rings: towards a mechanistic understanding of isotope fractionation and mixing processes from the leaves to the wood. *Tree Physiology*, 34(8), 796–818.
- Gessler, A. & Ferrio, J.P. (2022) Postphotosynthetic fractionation in leaves, phloem and stem. In: Siegwolf, R.T.W., Brooks, J.R., Roden, J. & Saurer, M., (Eds.) *Stable isotopes in tree rings*. Springer. pp. 381–396.
- Gessler, A., Keitel, C., Kodama, N., Weston, C., Winters, A.J., Keith, H. et al. (2007) $\delta^{13}\text{C}$ of organic matter transported from the leaves to the roots in *Eucalyptus delegatensis*: short-term variations and relation to respired CO_2 . *Functional Plant Biology*, 34(8), 692–706.
- Gessler, A., Rennenberg, H. & Keitel, C. (2004) Stable isotope composition of organic compounds transported in the phloem of European beech - evaluation of different methods of phloem sap collection and assessment of gradients in carbon isotope composition during leaf-to-stem transport. *Plant Biology*, 6, 721–729.
- Gessler, A., Tcherkez, G., Karyanto, O., Keitel, C., Ferrio, J.P., Ghashghaie, J. et al. (2009) On the metabolic origin of the carbon isotope composition of CO_2 evolved from darkened light-acclimated leaves in *Ricinus communis*. *New Phytologist*, 181, 374–386.
- Ghashghaie, J., Badeck, F.W., Lanigan, G., Nogués, S., Tcherkez, G., Deléens, E. et al. (2003) Carbon isotope fractionation during dark respiration and photorespiration in C_3 plants. *Phytochemistry Reviews*, 2, 145–161.
- Gilbert, A., Robins, R.J., Remaud, G.S., & Tcherkez, G.G.B. (2012) Intramolecular ^{13}C pattern in hexoses from autotrophic and heterotrophic C_3 plant tissues. *Proceedings of the National Academy of Sciences of the United States of America*, 109, 18204–18209.
- Gilbert, A., Silvestre, V., Robins, R.J., Tcherkez, G. & Remaud, G.S. (2011) A ^{13}C NMR spectrometric method for the determination of intramolecular $\delta^{13}\text{C}$ values in fructose from plant sucrose samples. *New Phytologist*, 191(2), 579–588.
- Gleixner, G., Danier, H.-J., Werner, R.A. & Schmidt, H.-L. (1993) Correlations between the ^{13}C content of primary and secondary plant products in different cell compartments and that in decomposing basidiomycetes. *Plant Physiology*, 102, 1287–1290.
- Gleixner, G. & Schmidt, H.-L. (1997) Carbon isotope effects on the fructose-1,6-bisphosphate aldolase reaction, origin for non-statistical ^{13}C distributions in carbohydrates. *Journal of Biological Chemistry*, 272(9), 5382–5387.
- Gleixner, G., Scrimgeour, C., Schmidt, H.-L. & Viola, R. (1998) Stable isotope distribution in the major metabolites of source and sink organs of *Solanum tuberosum* L.: a powerful tool in the study of metabolic partitioning in intact plants. *Planta*, 207, 241–245.
- Helama, S., Arppe, L., Timonen, M., Mielikäinen, K. & Oinonen, M. (2018) A 7.5 ka chronology of stable carbon isotopes from tree rings with implications for their use in palaeo-cloud reconstruction. *Global and Planetary Change*, 170, 20–33.
- Helle, G. & Schleser, G.H. (2004) Beyond CO_2 -fixation by Rubisco—an interpretation of $^{13}\text{C}/^{12}\text{C}$ variations in tree rings from novel intra-seasonal studies on broad-leaf trees. *Plant, Cell and Environment*, 27, 367–380.
- Hijaz, F. & Killiny, N. (2014) Collection and chemical composition of phloem sap from *Citrus sinensis* L. Osbeck (sweet orange). *PLoS One*, 9(7), e101830.

- Hinckley, T.M. & Lassoie, J.P. (1981) Radial growth in conifers and deciduous trees: a comparison. *Mitteilungen der Forstlichen Bundes Versuchsanstalt Wien*, 142, 17–56.
- Hobbie, E.A., Sánchez, F.S. & Rygielwicz, P.T. (2012) Controls of isotopic patterns in saprotrophic and ectomycorrhizal fungi. *Soil Biology and Biochemistry*, 48, 60–68.
- Högberg, M.N., Briones, M.J.I., Keel, S.G., Metcalfe, D.B., Campbell, C., Midwood, A.J. et al. (2010) Quantification of effects of season and nitrogen supply on tree below-ground carbon transfer to ectomycorrhizal fungi and other soil organisms in a boreal pine forest. *New Phytologist*, 187(2), 485–493.
- Jäggi, M., Saurer, M., Fuhrer, J. & Siegwolf, R. (2002) The relationship between the stable carbon isotope composition of needle bulk material, starch, and tree rings in *Picea abies*. *Oecologia*, 131, 325–332.
- Jammer, A., Gasperl, A., Luschin-Ebengreuth, N., Heyneke, E., Chu, H., Cantero-Navarro, E. et al. (2015) Simple and robust determination of the activity signature of key carbohydrate metabolism enzymes for physiological phenotyping in model and crop plants. *Journal of Experimental Botany*, 66(18), 5531–5542.
- Janecka, K., Kaczka, R.J., Gärtner, H., Harvey, J.E. & Treydte, K. (2020) Compression wood has a minor effect on the climate signal in tree-ring stable isotope records of montane Norway spruce. *Tree Physiology*, 40(8), 1014–1028.
- Johnson, D.W. & Ball, J.T. (1996) Interactions between CO_2 and nitrogen in forests: can we extrapolate from the seedling to the stand level? In: Koch, G.W. & Mooney, H.A. (Eds.) *Carbon dioxide and terrestrial ecosystems*. Academic Press, pp. 283–297.
- Jyske, T., Mäkinen, H., Kallikokki, T. & Nöjd, P. (2014) Intra-annual tracheid production of Norway spruce and Scots pine across a latitudinal gradient in Finland. *Agricultural and Forest Meteorology*, 194, 241–254.
- Kagawa, A., Sugimoto, A. & Maximov, T.C. (2006) Seasonal course of translocation, storage and remobilization of ^{13}C pulse-labeled photoassimilate in naturally growing *Larix gmelinii* saplings. *New Phytologist*, 171, 793–804.
- Kress, A., Saurer, M., Siegwolf, R.T.W., Frank, D.C., Esper, J. & Bugmann, H. (2010) A 350 year drought reconstruction from Alpine tree ring stable isotopes. *Global Biogeochemical Cycles*, 24(2).
- Kress, A., Young, G.H.F., Saurer, M., Loader, N.J., Siegwolf, R.T.W. & McCarroll, D. (2009) Stable isotope coherence in the earlywood and latewood of tree-line conifers. *Chemical Geology*, 268(1), 52–57.
- Krummen, M., Hilkert, A.W., Juchelka, D., Duhr, A., Schlüter, H.J. & Pesch, R. (2004) A new concept for isotope ratio monitoring liquid chromatography/mass spectrometry. *Rapid Communications in Mass Spectrometry*, 18(19), 2260–2266.
- Kurkela, T., Drenkhan, R., Vuorinen, M. & Hanso, M. (2009) Growth response of young Scots pines to needle loss assessed from productive foliage. *Forestry Studies/Metsanduslikud Uurimused*, 50, 5–22.
- Leavitt, S.W. & Long, A. (1984) Sampling strategy for stable carbon isotope analysis of tree rings in pine. *Nature*, 311(5982), 145–147.
- Lehmann, M.M., Ghiasi, S., George, G.M., Cormier, M.-A., Gessler, A., Saurer, M. et al. (2019) Influence of starch deficiency on photosynthetic and post-photosynthetic carbon isotope fractionations. *Journal of Experimental Botany*, 70, 1829–1841.
- Leppä, K., Tang, Y., Ogée, J., Launiainen, S., Kahmen, A., Kolari, P. et al. (2022) Explicitly accounting for needle sugar pool size crucial for predicting intra-seasonal dynamics of needle carbohydrates $\delta^{18}\text{O}$ and $\delta^{13}\text{C}$. *New Phytologist*, 236(6), 2044–2060.
- Lintunen, A., Paljakka, T., Jyske, T., Peltoniemi, M., Sterck, F., von Arx, G. et al. (2016) Osmolality and non-structural carbohydrate composition in the secondary phloem of trees across a latitudinal gradient in Europe. *Frontiers in Plant Science*, 7, 726.
- Livingston, N.J. & Spittlehouse, D.L. (1996) Carbon isotope fractionation in tree ring early and late wood in relation to intra-growing season water balance. *Plant, Cell and Environment*, 19, 768–774.
- Loader, N.J., McCarroll, D., Barker, S., Jalkanen, R. & Grudd, H. (2017) Inter-annual carbon isotope analysis of tree-rings by laser ablation. *Chemical Geology*, 466, 323–326.
- Loader, N.J., Robertson, I., Barker, A.C., Switsur, V.R. & Waterhouse, J.S. (1997) An improved method for the batch processing of small whole wood samples to α -cellulose. *Chemical Geology*, 136, 313–317.
- Mathias, J.M. & Thomas, R.B. (2021) Global tree intrinsic water use efficiency is enhanced by increased atmospheric CO_2 and modulated by climate and plant functional types. *Proceedings of the National Academy of Sciences*, 118(7), e2014286118.
- Maunoury-Danger, F., Bathellier, C., Laurette, J., Fresneau, C., Ghashghaie, J., Damesin, C. et al. (2009) Is there any $^{12}\text{C}/^{13}\text{C}$ fractionation during starch remobilisation and sucrose export in potato tubers? *Rapid Communications in Mass Spectrometry*, 23(16), 2527–2533.
- Mauve, C., Bleton, J., Bathellier, C., Lelarge-Trouverie, C., Guérard, F., Ghashghaie, J. et al. (2009) Kinetic $^{12}\text{C}/^{13}\text{C}$ isotope fractionation by invertase: evidence for a small in vitro isotope effect and comparison of two techniques for the isotopic analysis of carbohydrates. *Rapid Communications in Mass Spectrometry*, 23(16), 2499–2506.
- Merchant, A., Peuke, A.D., Keitel, C., Macfarlane, C., Warren, C.R. & Adams, M.A. (2010) Phloem sap and leaf $\delta^{13}\text{C}$, carbohydrates, and amino acid concentrations in *Eucalyptus globulus* change systematically according to flooding and water deficit treatment. *Journal of Experimental Botany*, 61(6), 1785–1793.
- Michelot, A., Eglin, T., Dufrière, E., Lelarge-Trouverie, C. & Damesin, C. (2011) Comparison of seasonal variations in water-use efficiency calculated from the carbon isotope composition of tree rings and flux data in a temperate forest. *Plant, Cell & Environment*, 34(2), 230–234.
- Monson, R.K., Szejner, P., Belmecheri, S., Morino, K.A. & Wright, W.E. (2018) Finding the seasons in tree ring stable isotope ratios. *American Journal of Botany*, 105, 819–821.
- Nguyen, Q.A., Luan, S., Wi, S.G., Bae, H., Lee, D.S. & Bae, H.J. (2016) Pronounced phenotypic changes in transgenic tobacco plants overexpressing sucrose synthase may reveal a novel sugar signaling pathway. *Frontiers in Plant Science*, 6, 1216.
- Panek, J.A. & Waring, R.H. (1997) Stable carbon isotopes as indicators of limitations to forest growth imposed by climate stress. *Ecological Applications*, 7(3), 854–863.
- Pérez-de-Lis, G., Rathgeber, C.B.K., Fernández-de-Uña, L. & Ponton, S. (2022) Cutting tree rings into time slices: how intra-annual dynamics of wood formation help decipher the space-for-time conversion. *New Phytologist*, 233(3), 1520–1534.
- Rende, U., Wang, W., Gandla, M.L., Jönsson, L.J. & Niittylä, T. (2017) Cytosolic invertase contributes to the supply of substrate for cellulose biosynthesis in developing wood. *New Phytologist*, 214(2), 796–807.
- Rinne, K.T., Boettger, T., Loader, N.J., Robertson, I., Switsur, V.R. & Waterhouse, J.S. (2005) On the purification of α -cellulose from resinous wood for stable isotope (H, C and O) analysis. *Chemical Geology*, 222, 75–82.
- Rinne, K.T., Loader, N.J., Switsur, V.R., Treydte, K.S. & Waterhouse, J.S. (2010) Investigating the influence of sulphur dioxide (SO_2) on the stable isotope ratios ($\delta^{13}\text{C}$ and $\delta^{18}\text{O}$) of tree rings. *Geochimica et Cosmochimica Acta*, 74(8), 2327–2339.
- Rinne, K.T., Saurer, M., Kirilyanov, A.V., Bryukhanova, M.V., Prokushkin, A.S. & Sidorova, O.V.C. et al. (2015) Examining the response of needle carbohydrates from Siberian larch trees to climate using compound-specific $\delta^{13}\text{C}$ and concentration analyses. *Plant, Cell and Environment*, 38(11), 2340–2352.
- Rinne, K.T., Saurer, M., Kirilyanov, A.V., Loader, N.J., Bryukhanova, M.V., Werner, R.A. et al. (2015) The relationship between needle sugar carbon isotope ratios and tree rings of larch in Siberia. *Tree Physiology*, 35(11), 1192–1205.

- Rinne, K.T., Saurer, M., Streit, K. & Siegwolf, R.T.W. (2012) Evaluation of a liquid chromatography method for compound-specific $\delta^{13}\text{C}$ analysis of plant carbohydrates in alkaline media: compound-specific $\delta^{13}\text{C}$ analysis of plant carbohydrates in alkaline media. *Rapid Communications in Mass Spectrometry*, 26(18), 2173–2185.
- Rinne-Garmston, K.T., Helle, G., Lehmann, M., Sahlstedt, E., Schleucher, J. & Waterhouse, J. (2022) Newer developments in tree ring stable isotope methods. *Stable isotopes in tree rings: inferring physiological, climatic and environmental responses*, tree physiology. Springer. p. 773
- Robakowski, P. & Bielinis, E. (2017) Needle age dependence of photosynthesis along a light gradient within an *Abies alba* crown. *Acta Physiologiae Plantarum*, 39(3), 83.
- Rossi, S., Anfodillo, T. & Menardi, R. (2006) Trephor: a new tool for sampling microcores from tree stems. *IAWA Journal*, 27(1), 89–97.
- Ryhti, K., Schiestl-Aalto, P., Tang, Y., Rinne-Garmston, K.T., Ding, Y., Pumpanen, J. et al. (2022) Effects of variable temperature and moisture conditions on respiration and nonstructural carbohydrate dynamics of tree roots. *Agricultural and Forest Meteorology*, 323, 109040.
- Schiestl-Aalto, P., Stangl, Z.R., Tarvainen, L., Wallin, G., Marshall, J. & Mäkelä, A. (2021) Linking canopy-scale mesophyll conductance and phloem sugar $\delta^{13}\text{C}$ using empirical and modelling approaches. *New Phytologist*, 229(6), 3141–3155.
- Schleser, G.H. (1989) Investigations of the $\delta^{13}\text{C}$ pattern in leaves of *Fagus sylvatica* L. *Journal of Experimental Botany*, 41(226), 565–572.
- Schmidt, H.-L. & Gleixner, G. (1998) Carbon isotope effects on key reactions in plant metabolism and ^{13}C -patterns in natural compounds. In: Griffiths, H.G., (Ed.) *Stable isotopes*. BIOS Scientific Publisher. pp. 13–25.
- Schulze, B., Wirth, C., Linke, P., Brand, W.A., Kuhlmann, I., Horna, V. et al. (2004) Laser ablation-combustion-GC-IRMS—a new method for online analysis of intra-annual variation of $\delta^{13}\text{C}$ in tree rings. *Tree Physiology*, 24, 1193–1201.
- Schuster, W.S.F., Phillips, S.L., Sandquist, D.R. & Ehleringer, J.R. (1992) Heritability of carbon isotope discrimination in *Gutierrezia microcephala* (Asteraceae). *American Journal of Botany*, 79, 216–221.
- Sidorova, O.V.C., Lehmann, M.M., Siegwolf, R.T.W., Saurer, M., Fonti, M.V. & Schmid, L. et al. (2019) Compound-specific carbon isotope patterns in needles of conifer tree species from the Swiss National Park under recent climate change. *Plant Physiology and Biochemistry*, 139, 264–272.
- Sidorova, O.V.C., Lehmann, M., Saurer, M., Fonti, M., Siegwolf, R. & Bigler, C. (2018) Compound-specific carbon isotopes and concentrations of carbohydrates and organic acids as indicators of tree decline in mountain pine. *Forests*, 9(6), 363.
- Sidorova, O.V., Siegwolf, R.T.W., Saurer, M., NAurzbaev, M.M., Shashkin, A.V. & Vaganov, E.A. (2010) Spatial patterns of climatic changes in the Eurasian north reflected in Siberian larch tree-ring parameters and stable isotopes. *Global Change Biology*, 16(3), 1003–1018.
- Smith, M., Wild, B., Richter, A., Simonin, K. & Merchant, A. (2016) Carbon isotope composition of carbohydrates and polyols in leaf and phloem sap of *Phaseolus vulgaris* L. influences predictions of plant water use efficiency. *Plant and Cell Physiology*, 57(8), 1756–1766.
- Stein, O. & Granot, D. (2019) An overview of sucrose synthases in plants. *Frontiers in Plant Science*, 10, 95.
- Streit, K., Rinne, K.T., Hagedorn, F., Dawes, M.A., Saurer, M., Hoch, G. et al. (2013) Tracing fresh assimilates through *Larix decidua* exposed to elevated CO_2 and soil warming at the alpine treeline using compound-specific stable isotope analysis. *New Phytologist*, 197(3), 838–849.
- Tang, Y., Sahlstedt, E., Young, G., Schiestl-Aalto, P., Saurer, M., Kolari, P. et al. (2023) Estimating intra-seasonal intrinsic water-use efficiency from high-resolution tree-ring $\delta^{13}\text{C}$ data in boreal Scots pine forests. *New Phytologist*, 237(5), 1606–1619.
- Tang, Y., Schiestl-Aalto, P., Lehmann, M.M., Saurer, M., Sahlstedt, E., Kolari, P. et al. (2022) Estimating intra-seasonal photosynthetic discrimination and water use efficiency using $\delta^{13}\text{C}$ of leaf sucrose in Scots pine. *Journal of Experimental Botany*, 74(1), 321–335.
- Tang, Y., Schiestl-Aalto, P., Saurer, M., Sahlstedt, E., Kulmala, L., Kolari, P. et al. (2022) Tree organ growth and carbon allocation dynamics impact the magnitude and $\delta^{13}\text{C}$ signal of stem and soil CO_2 fluxes. *Tree Physiology*, 42, 2404–2418.
- Tcherkez, G., Mahé, A. & Hodges, M. (2011) (12)C/(13)C fractionations in plant primary metabolism. *Trends in Plant Science*, 16(9), 499–506.
- Tcherkez, G., Nogués, S., Bleton, J., Cornic, G., Badeck, F. & Ghashghaie, J. (2003) Metabolic origin of carbon isotope composition of leaf dark-respired CO_2 in French bean. *Plant Physiology*, 131(1), 237–244.
- Terwilliger, V.J., Kitajima, K., Le Roux-Swarthout, D.J., Mulkey, S. & Wright, S.J. (2001) Influences of heterotrophic and autotrophic resource use on carbon and hydrogen isotopic compositions of tropical tree leaves. *Isotopes in Environmental and Health Studies*, 37, 133–160.
- Timell, T.E. (1986) Chemical properties of compression wood. *Compression wood in gymnosperms*. Springer-Verlag.
- Vitali, V., Martínez-Sancho, E., Treydte, K., Andreu-Hayles, L., Dorado-Liñán, I., Gutierrez, E. et al. (2022) The unknown third—hydrogen isotopes in tree-ring cellulose across Europe. *Science of the Total Environment*, 813, 152281.
- Walia, A., Guy, R.D. & White, B. (2010) Carbon isotope discrimination in western hemlock and its relationship to mineral nutrition and growth. *Tree Physiology*, 30(6), 728–740.
- Wanek, W., Heintel, S. & Richter, A. (2001) Preparation of starch and other carbon fractions from higher plant leaves for stable carbon isotope analysis. *Rapid Communications in Mass Spectrometry*, 15, 1136–1140.
- Werner, C. & Gessler, A. (2011) Diel variations in the carbon isotope composition of respired CO_2 and associated carbon sources: a review of dynamics and mechanisms. *Biogeosciences*, 8(9), 2437–2459.
- Werner, R.A. & Brand, W.A. (2001) Referencing strategies and techniques in stable isotope ratio analysis. *Rapid Communications in Mass Spectrometry*, 15(7), 501–519.
- Wingate, L., Ogée, J., Burrell, R., Bosc, A., Devaux, M., Grace, J. et al. (2010) Photosynthetic carbon isotope discrimination and its relationship to the carbon isotope signals of stem, soil and ecosystem respiration. *New Phytologist*, 188(2), 576–589.
- Zweifel, R., Sterck, F., Braun, S., Buchmann, N., Eugster, W., Gessler, A. et al. (2021) Why trees grow at night. *New Phytologist*, 231(6), 2174–2185.

SUPPORTING INFORMATION

Additional supporting information can be found online in the Supporting Information section at the end of this article.

How to cite this article: Rinne-Garmston, K.T., Tang, Y., Sahlstedt, E., Adamczyk, B., Saurer, M., Salmon, Y. et al. (2023) Drivers of intra-seasonal $\delta^{13}\text{C}$ signal in tree-rings of *Pinus sylvestris* as indicated by compound-specific and laser ablation isotope analysis. *Plant, Cell & Environment*, 1–18. <https://doi.org/10.1111/pce.14636>